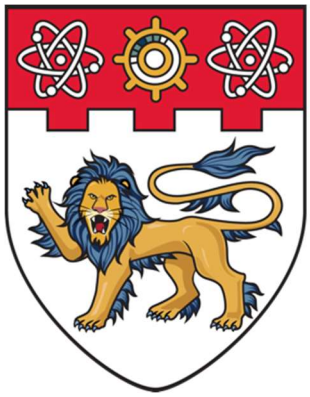

NANYANG TECHNOLOGICAL UNIVERSITY
SINGAPORE

# EFFECT OF MICROBIAL TRANSGLUTAMINASE-INDUCED CROSSLINKING ON RHEOLOGICAL PROPERTIES OF GELATIN METHACRYLOYL INK FOR 3D PRINTING

**ZHOU MIAOMIAO**

**SCHOOL OF MATERIALS SCIENCE AND ENGINEERING**

**2018**

# EFFECT OF MICROBIAL TRANSGLUTAMINASE-INDUCED CROSSLINKING ON RHEOLOGICAL PROPERTIES OF GELATIN METHACRYLOYL INK FOR 3D PRINTING

**ZHOU MIAOMIAO**

SCHOOL OF MATERIALS SCIENCE AND ENGINEERING

A thesis submitted to the Nanyang Technological University
in partial fulfilment of the requirement for the degree of
Master of Engineering

**2018**

# Statement of Originality

I hereby certify that the work embodied in this thesis is the result of original research and has not been submitted for a higher degree to any other University or Institution.

. ……2017.8.24. . . . . .  . . . . 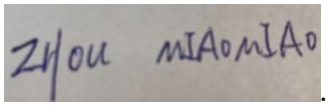 . ... . . ..

Date  ZHOU MIAOMIAO

## Abstract

3D bioprinting provides an efficient mean to fabricate 3D cellular constructs with defined shape and controlled spatial organization. Despite some remarkable successes, it still remains challenging to develop a bioink to meet the requirements (cell-compatibility, printability, structural stability post printing) for printing. Herein, this thesis presents a new strategy for bioprinting of photo crosslinkable Gelatin methacryloyl (GelMA) through enzymatic crosslinking reactions. $Ca^{2+}$-independent microbial transglutaminase (MTGase) catalyzed covalent bond formation between chains of GelMA and rheological properties were first optimized. A secondary post-printing crosslinking step (photo crosslinking) was then introduced to ensure long term stability of the printed structure for subsequent cell studies. Cells encapsulated in the printed structure were viable for at least 7 days indicating excellent biocompatibility. This strategy for printing of cell-laden photo crosslinkable GelMA may find valuable application in organ printing and tissue engineering.

## Acknowledgements

I would like to extend my deepest gratitude to my supervisor, Associate Professor Tan Lay Poh from Nanyang Technological University School of Materials Science and Engineering (MSE NTU). Prof. Tan has given me valuable guidance throughout my every stage of study.

I would also like to thank Dr Lee Bae Hoon and Dr Tan Yu Jun for their advice and guidance on material synthesis and 3D printing. Finally, I wish to extend my thanks to my colleagues in the Biomaterials and Organic Service laboratory.

# Table of Contents

# Table Captions

# Figure Captions

# Abbreviations

| | |
|---|---|
| GelMA | Gelatin Methacryloyl |
| MTGase | Microbial Transglutaminase |
| OPTN | Organ Procurement and Transplantation Network |
| NMR | Nuclear Magnetic Resonance |
| RGD | Arginine-Glycine-Aspartic Acid |
| MMP | Matrix Metalloproteinase |
| UCST | Upper Critical Solution Temperature |
| LCST | Lower Critical Solution Temperature |
| MAAnh | Methacrylic Anhydride |
| I2959 | Irgacure 2959 |
| ECM | Extracellular Matrix |
| DM | Degree of Methacryloylation |
| CB | Carbonate-Bicarbonate |
| DMEM | Dulbecco's Modified Eagle's Medium |
| FBS | Fetal Bovine Serum |
| ABAM | Antibiotic-Antimycotic |

# Chapter 1

# Introduction

*In this chapter, a brief introduction is summarized for this thesis. Firstly, the background and motivation (Section 1.1) for development of 3D printing material are described followed by the objectives of this thesis (Section 1.2). Subsequently, the organization of this thesis is outlined in sequence (Section 1.3). In the end, the finds and outcomes are included to present the main contributions of this work.*

## 1.1 Background and motivation

Organ shortage [1] calls a great need for the development of new biological substitutes. Tissue engineering has emerged as an attractive method to meet this need. The classic tissue engineering strategy is to seed specific cells isolated from a biopsy onto a three-dimensional (3D) scaffold, occasionally incorporating growth factors, to provide a temporal support for cell proliferation, differentiation, and eventually formation of neotissue [2]. One major limitation of this strategy is the lack of precision in cell placement due to manual cell seeding; it is difficult to place different cell types at certain position depending on the type and function of a tissue [3]. To overcome this drawback, an automated and precise technology known as 3D bioprinting, has gained scientists' interest in recent years. It is a computer-controlled process to produce 3D constructs layer-by-layer, in which cells mixed with biomaterials can be distributed in a certain position [4]. This direct method makes it an attractive tool for the development of 3D organised cellular constructs with special biological and mechanical properties [5].

One major challenge of 3D bioprinting is to develop a bioink to meet a repertoire of characteristics suitable for printing. The bioink should have suitable physiochemical properties, such as shear thinning, high viscosity, as well as post-printing structural stability [6, 7]. Besides, the bioink can provide a desirable environment for cells to encapsulate, migrate, proliferate and differentiate [8]. Hydrogels exert great potential as bioink due to their cell-encapsulating ability and mimicking of the physical and chemical properties of the extracellular matrix (ECM) [9]. The difficulty lies in the delicate balance between printability and biological properties of hydrogels towards 3D bioprinting. Increasing the polymer concentration results in a highly viscous hydrogel precursor and a quick gelation into a crosslinked hydrogel, which provides good printability and high shape fidelity [10, 11], but a dense polymer network can inhibit formation of new ECM and matrix remodelling as well as cell migration [12, 13]. Therefore, development of a hydrogel system with appropriate balance of printability and cell support will promote hydrogel application in 3D bioprinting.

Large numbers of natural or synthetic derived hydrogels have been studied for 3D bioprinting such as alginate [14], collagen [15], gelatin [16] and poly(ethylene glycol) diacrylate [17]. Among those materials, gelatin is an attractive material with biological cues containing cell adhesion motifs (arginine-glycine-aspartic acid (RGD) sequences) and target sites for matrix metalloproteinase (MMP) in cell remodelling and degradation [18]. The thermally sensitive ability of gelatin can support the printing process [19-22]. Moreover, gelatin can be modified with methacrylamide and a minority of methacrylate groups, resulting in a photo-crosslinkable material—gelatin methacryloyl (GelMA) [23]. GelMA retains biofunctionality from gelatin [18] and its photo-crosslinkable property enables quick formation of a covalently crosslinked hydrogel and maintaining the printed construct permanently; thus become stable under physiological temperature [24].

GelMA has been demonstrated as a suitable bioink for 3D bioprinting. Printing GelMA requires relatively high polymer concentrations due to low viscosity at 37 °C [24]; however the previous work has shown that the high polymer concentration could compromise cell viability [24-26]. Nichol et al. studied cell viability of NIH 3T3 fibroblasts encapsulated in 5%-15% GelMA and high cell viability (>80%) was generally observed in below 10% GelMA [27]. Additionally, to improve the printability of GelMA, precise control of the nozzle temperature and cooling down the platform have been conducted to successfully print GelMA but the hardware became important [28]. Thus, development of a smart system with improved rheological properties is imperative for using GelMA in 3D bioprinting.

In this work, an enzymatic crosslinking process-triggered by a $Ca^{2+}$-independent microbial transglutaminase (MTGase), a nontoxic crosslinker with high specific activity [29], was introduced to catalyse the isopeptide formation between the γ-carboxamides of glutamine residues and ε-primary amino of lysine residues in chains of GelMA [30]. We hypothesize that this enzymatic crosslinking method could improve the rheological properties and printability. We examined the rheological properties and printability of 10% GelMA solution treated with MTGase as well as the cell viability of printed structures.

## 1.2 Objectives

The aim of this work is to investigate the effect of MTGase-induced crosslinking on rheological properties and printability of GelMA. GelMA was synthesized by chemical modification of gelatin. The rheological properties of GelMA were tailored through manipulating MTGase concentration and incubation time. Based on rheology study, a suitable bioink was selected for further printability assessment using commercially available bioprinter. Following that, the in situ cell viability of the printed constructs was conducted to examine the influence of printing process and the biocompatibility of the bioink.

The objectives of the research are specified as:

1. Synthesis and characterization of GelMA
2. Rheological characterization of GelMA treated with MTGase
3. Printability test of GelMA treated with MTGase
4. Cell viability evaluation

## 1.3 Dissertation Overview

This thesis consists of the following five chapters:

*Chapter 1* gives a brief introduction of development of 3D bioprinting material. The need for development of a suitable bioink has been described. Among different kinds of bioink, GelMA is an attractive and promising bioink due to its superior biological properties. Nevertheless, the poor rheological properties such as low viscosity and slow gelation limit its further use in 3D bioprinting. In our work, an enzymatic crosslinking triggered by microbial transglutaminase was introduced for partially covalent bonding the GelMA chains and thus improved its rheological properties and printability.

*Chapter 2* provides a wide range of literature review for better understanding of the basic knowledge on 3D bioprinting techniques and materials. Three common 3D bioprinting

techniques are briefly described. The advantages and disadvantages of those three techniques are summarized, which provides a guidance for choosing a proper printing technique for targeted research purpose. As following, some commonly used biomaterials in 3D bioprinting are introduced. Besides, the hydrogel properties required for bioprinting are summarized from literatures. Finally, the existing challenge in 3D bioprinting is presented.

*Chapter 3* describes the experimental design, materials and method used in this thesis.

*Chapter 4* focus on the effect of MTGase-induced crosslinking on rheological properties, printability and cell viability of GelMA. GelMA was mixed with different MTGase concentration. Then, the rheological properties of GelMA were examined with different MTGase concentration at different incubation time. Based on rheological study, an optimized mixture was selected for 3D bioprinting. A cell-laden structure was constructed followed by cell viability study.

*Chapter 5* gives a brief conclusion of the overall thesis and provides some guides for future research.

## 1.4 Findings and Outcomes/Originality

The main objective of this thesis is to investigate the effect of MTGase induced crosslinking on rheological properties of GelMA towards 3D bioprinting. GelMA has been successfully synthesized. The rheological properties of GelMA can be tailored by manipulating MTGase concentration and incubation time. The printability of the MTGase-treated GelMA has been significantly enhanced owing to the improved viscosity under shear rate 100 s-1 from 5.9 mPa•s to 5776.0 mPa•s after enzymatic treatment, as shown in Figure 11. It should also be noted that the reaction doesn't affect the shear thinning behavior of the GelMA, both treated and native GelMA possessed power law index of 0.542 and 0.999, respectively. Shear thinning hydrogel is attractive for bioprinting due to its stress-relaxation property [31]. Meanwhile, the sol-gel transition temperature of GelMA

with MTGase treatment is raised to room temperature (25 ℃), resulting in a gel-like character under printing condition (room temperature 25℃) and providing a good shape fidelity. Cell culture with C2C12 cells show significant cell elongation after 3 days and high cell viability as indicated by live-dead staining. C2C12 elongation is an indication of the healthy state of cells [32].

# Chapter 2

## Literature Review

*In this chapter, a wide range of literature review has been provided. Firstly, three common 3D bioprinting techniques are briefly described and compared followed by introducing some commonly used biomaterials in 3D bioprinting. Besides, the hydrogel properties required for bioprinting are summarized from literatures. Finally, the existing challenge in 3D bioprinting is presented.*

## 2.1 Background

### 2.1.1 Emergence of tissue engineering

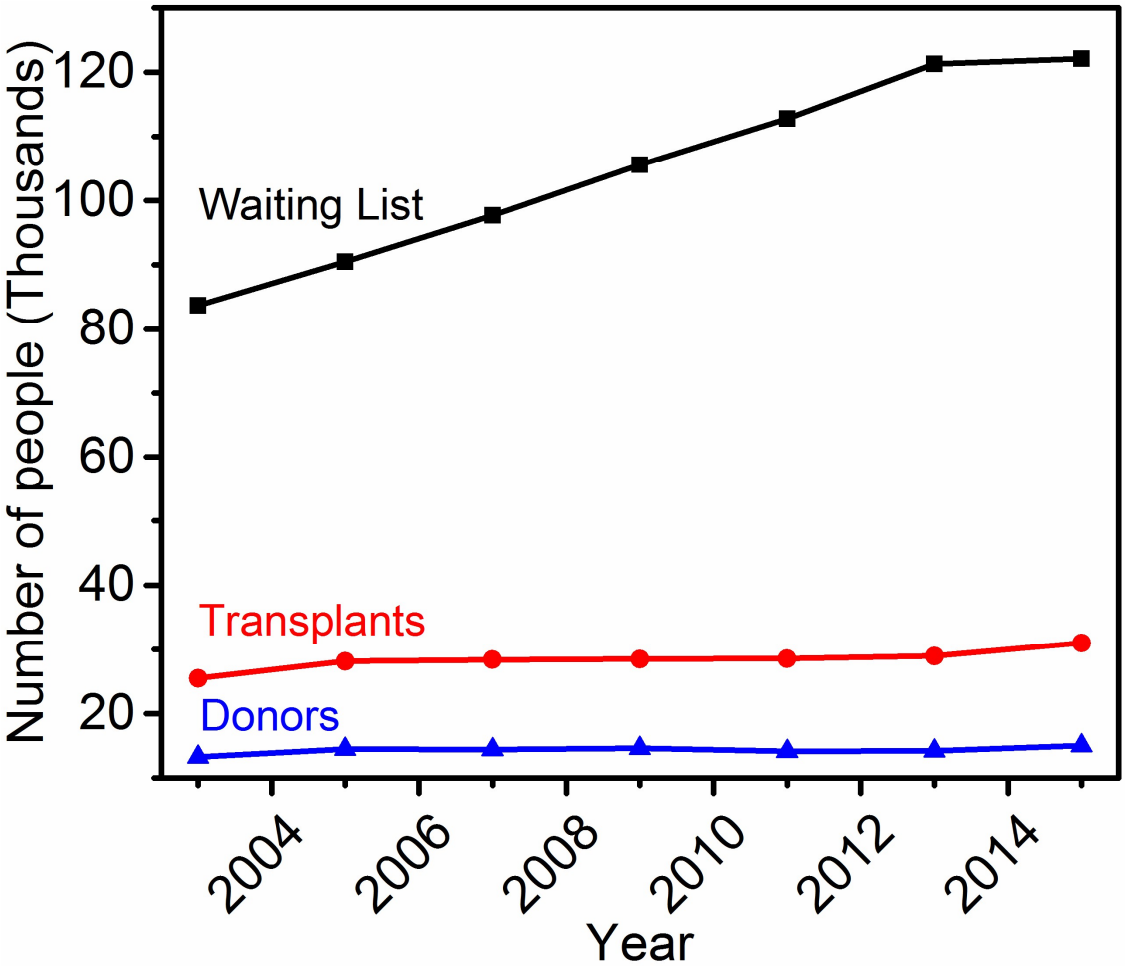


Figure 1. Organ transplants, donors and waiting list. Derived from OPTN data from 2003 to 2015.

Organ and tissue loss resulting from an injury or other types of damage is a major health problem around the world. Success in transplantation of organs provides a suitable remedy for patients with impaired organs. Despite being a major therapy, severe constraints were placed on the procedure, limiting the development of transplantation. The major issue is the access of sufficient organs to meet the existing demand. Figure 1 (derived from OPTN data) shows that in 2003 there were 83,731 on the waiting list, 25,473 transplants, 13,285

donors, which grew to 122,071 (1.46-fold increase) on the waiting list, 30,975 (1.22-fold increase) transplants, 15,068 (1.13-fold increase) donors in 2015. The gap between supply and demand keep widening. Many patients may die while waiting for organs. In addition, even if successfully transplanted with organs, patients are still facing a risk of chronic rejection over time. These problems call a great need to develop a novel method for alternative to transplantation.

Thus, tissue engineering has emerged. It combines the principles of engineering and life sciences to construct biological substitutes for maintaining, restoring or improving tissue or organs [33]. It enables cells donated by the patients to be used to reconstruct or repair tissue or organs free of immune rejection and considering as a promising technology to solve organ shortage crisis. Since its birth in the early 1970s, tissue engineering has covered large numbers of human organs, ranging from single organs such as skins [34] to complex organs such as liver [35].

### 2.1.2 Scaffolds for tissue engineering

The classic tissue engineering strategy (Figure 2) is to seed specific cells isolated from a biopsy onto a three-dimensional (3D) scaffold, occasionally incorporating growth factors, to provide a temporal support for cell proliferation and differentiation, eventually formation of neotissue [2]. The fate of cells seeded within the scaffold structures can be influenced by not only the selection of scaffold material but also the architectures of the scaffold such pore size, shape, and pore interconnection [36]. The material can be selected from synthetic or natural polymers such as peptides, proteins and hydrogels to produce scaffolds [37]. A scaffold with high porosity, well-interconnected pore structures, and consistent pore size and shape will be preferred for cell migration and infiltration [38], and those characteristics can be largely determined by the scaffold fabrication techniques.

There are various techniques that have been developed for scaffold fabrication over the past 40 years. Conventional fabrication techniques include fiber bonding, particulate leaching, solvent casting, melt moulding, membrane lamination, and freeze drying [39].

Though those techniques have brought great success in tissue engineering, there are still some limitations. One major drawback is that it cannot allow for fabrication of scaffold with homogenous pore shape, pore interconnectivity and cannot precisely control scaffold geometries [3]. For example, scaffolds produced by freeze drying are interconnected but heterogeneous due to the random freezing kinetics [40]. Other reported limitation of those techniques is the lack of precision in cell placement due to the inaccuracies of seeding cells by hand; it is difficult to place different cell types at certain position according to the type and function of tissue [41]. To overcome this drawback, 3D printing (known as additive manufacturing, solid free-form fabrication, or rapid prototyping) that is more design-dependent has gain researchers' interest in tissue engineering.

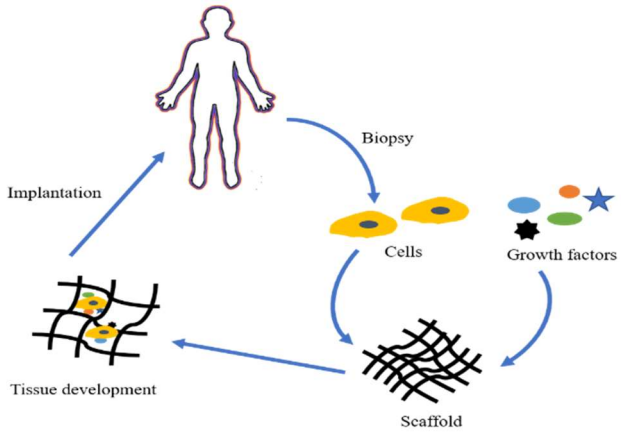


Figure 2. Overview of tissue engineering strategy.

## 2.2 Bioprinting techniques

3D printing was introduced by Charles Hull in 1986 when he developed a prototype system based on a process known as stereolithography, in which solid objects were made by successively printing a curable material layer-by-layer [42]. 3D bioprinting is an extension of 3D printing, which enables patterning and assembling biological materials such as biomolecules and cells into 3D scaffolds [43]. It is computer-controlled process that reads in data from CAD drawings and produces 3D constructs layer-by-layer, in which cells mixed with biomaterials can be distributed in a certain position. This direct method for fabricating 3D constructs makes it an attractive tool for construction of 3D complex living tissue with special biological and mechanical properties [5]. Multiple bioadditive

bioprinting techniques, including laser-based writing [44], inkjet-based [45], and extrusion-based deposition [46], are used to develop tissue-engineered constructs. Figure 3 summarizes existing bioprinting techniques that are discussed extensively next sections.

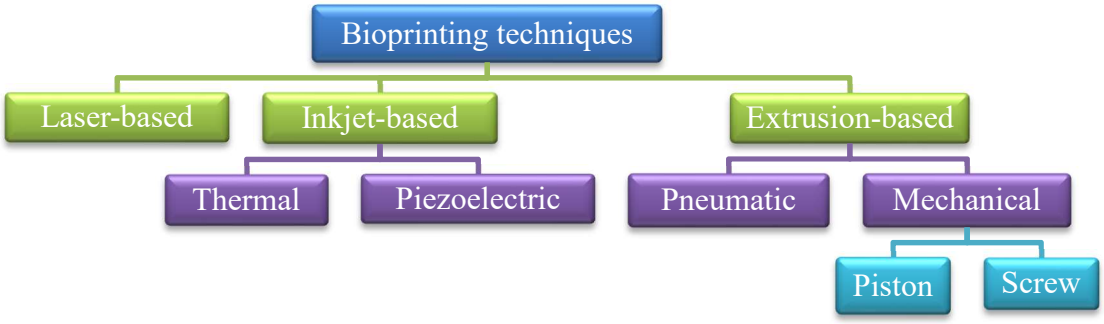


Figure 3. Classification of bioprinting techniques.

### 2.2.1 Inkjet bioprinting

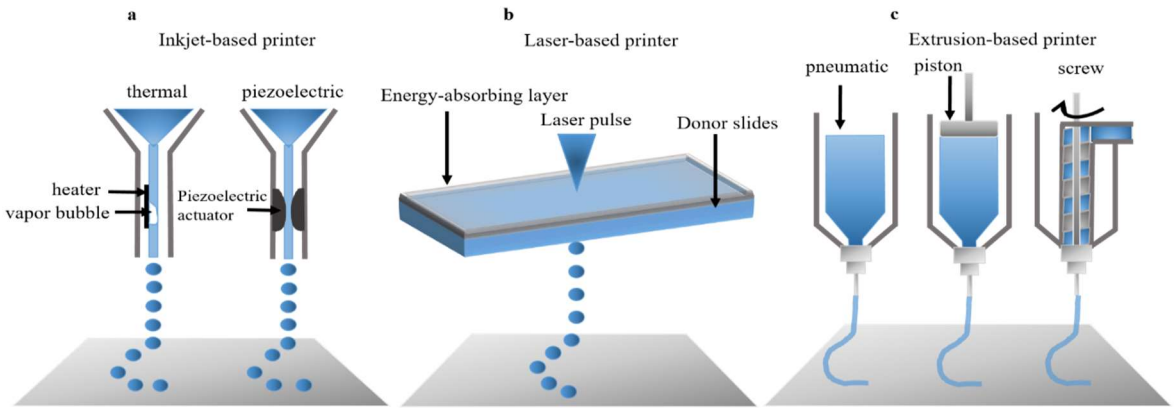


Figure 4. Bioprinting techniques including (a) inkjet-based printer; (b) laser-baes printer; (c) extrusion-based printer (Taken from [5]).

Inkjet printer was introduced for biological applications in the early 2000s. In this technique, biological materials in the cartridge are printed in the form of droplets, normally forced by thermal or piezoelectric forces (Figure 4a). The principle of thermal inkjet printing (Figure 4a) is that the formation and collapse of the bubble vaporized by a heating elements generates a pulse to force droplets from the print head with various volumes from 10 to 150 pL [47]. Piezoelectric inkjet printer (Figure 4a) adapts a piezoelectric actuator to generate acoustic wave to break the liquid into droplets and force it through the nozzle [5].

### 2.2.2 Laser printing

The first laser printer used for bioprinting applications was introduced in 1999 by Odde and Renn as a 2D ink-based printers [48]. Laser energy is the most important component in this technology, which is utilised to control and guide biological materials deposition. Figure 4b shows a schematic of laser-based printing. A typical set-up is comprised of a focused laser beam, a donor slide comprising a "ribbon" structure that is coated with an energy-absorbing layer on the top and a layer of biological materials on the bottom. A bubble is generated in the energy-absorbing layer where the focused laser beam is absorbed. This bubble produces a gas pressure to push the biological materials to the collector substrate.

### 2.2.3 Extrusion printing

Extrusion bioprinting is another bioprinting technique that is commonly used for creating living tissue constructs. In this technology, materials are extruded by robotic control. The most common dispensing system are pneumatic or mechanical (piston or screw)-driven system (Figure 4c).

Table 1 summarizes the requirement for comparison of some bioink parameter in the three types of bioprinter is summarized in the. Generally, inkjet-based and laser-based printing can provide high spatial resolution, ranging from 10-50 μm and 3-200 μm, respectively while extrusion-based system has a relative low resolution ranging from 200-1000 μm [7]. However, for constructing larger 3D structures, extrusion-based printer has an advantage over inkjet-based printer and laser-based printer. High cell density is not allowed in inkjet-based printer and laser-based printer due to its possibility to clogging of the nozzle.

Table 1 Comparison of bioprinter types [Taken from ref. [5]]

| | Bioprinter type | | |
|---|---|---|---|
| | Inkjet | Microextrusion | Laser assisted |
| Material viscosities | 3.5–12 mPa/s | 30 mPa/s to >6 x $10^7$ mPa/s | 1–300 mPa/s |
| Gelation methods | Chemical, photo-crosslinking | Chemical, photo-crosslinking, sheer thinning, temperature | Chemical, photo-crosslinking |
| Preparation time | Low | Low to medium | Medium to high |
| Print speed | Fast (1–10,000 droplets per second) | Slow (10–50 µm/s) | Medium-fast (200–1,600 mm/s) |
| Resolution or droplet size | <1 pl to >300 pl droplets, 50 µm wide | 5 µm to millimeters wide | Microscale resolution |
| Cell viability | >85% | 40–80% | >95% |
| Cell densities | Low, <$10^6$ cells/ml | High, cell spheroids | Medium, $10^8$ cells/ml |
| Printer cost | Low | Medium | High |

## 2.3 Hydrogels for bioprinting

In the 3D bioprinting, cells and bioactive molecules are printed as "bioinks," which should have cell compatibility to provide a desirable environment for cell adhesion and proliferation [8]. Hydrogel is an attractive material because its hydrophilicity and ability to mimic many characteristics of natural ECM [9]. A hydrogel is a three-dimensional network through crosslinking polymer chains either physically or chemically. Due to the cross-liked meshwork, up to 99% of water or biological fluid can be absorbed into the structure [49]. Before forming three-dimensional meshwork, cells can be added into this aqueous solution and then be crosslinked to form a cell-laden hydrogel. Many hydrogels have the potential for the application in 3D bioprinting including natural origin and synthetic derived polymer.

### 2.3.1 Natural polymers

#### *2.3.1.1 Collagen*

Collagen has been widely used in tissue engineering because it is the main constituent of natural extracellular matrix (ECM), which occupies 25% to 35% protein content in the body [50]. The thermos-and pH-sensitive properties of collagen can aid in constructing

three-dimensional structure. A viscoelastic hydrogel can be produced by adjusting the pH of precursors to 7.4 and incubating at 37 °C for 15-30min. Collagen hydrogel was once used in extrusion-type printer where it was mixed with bovine aortic endothelial cells. In this paper, Simith et al. were able to print a five-layer construct, in which cell viability was up to 86% [51].

#### *2.3.1.2 Gelatin/Gelatin methacryloyl*

Gelatin, a denatured product of collagen, contains many arginine-glycine-aspartic acid (RGD) sequences for cell attachment as well as the target sequences of matrix metalloproteinase(MMP) that are suitable for cell remodelling [23]. Different from native collagen, gelatin can be dissolved in pH neutral (7.4) solution while forming physical gels by lowering temperature through hydrogen bonding. This thermal responsive property can facilitate structure maintenance in 3D bioprinting. However, gelatin has melt temperature between 27 and 33 °C [52] and will melt under physiological temperatures which will limit its use in vivo application. To overcome this limitation, gelatin has reported to be chemical modified or mixed with other crosslinkable polymers.

For example, gelatin methacryloyl obtained from the chemical modification of gelatin with methacrylamide and a minority of methacrylate groups has retained biofunctionality from gelatin and its uv crosslinkable property enables forming covalently crosslinked hydrogels which are no longer temperature sensitive [24]. Nichol et al. studied cell viability of NIH 3T3 fibroblasts encapsulated in 5%-15% GelMA and high cell viability (>80%) was generally observed in below 10% GelMA [27]. However, its application in 3D bioprinting is inhibited by its poor rheological properties. Schuuirman et al. reported that the high concentration 20% GelMA formed droplets at the tip of needle at 37 due to low viscosity, while 2.4% hyaluronic acid (HA) was added to increase the viscosity and facilitate the filament deposition [24]. Billiet et al. have reported precise temperature control of nozzle to print cell-laden gelatin methacryloyl from 10% to 20% and constructed interconnect pore network [28]. However, the hardware modification become critical and there is a slightly collapse of structure of 10% GelMA due to slow thermal gelation.

#### *2.3.1.3 Alginate*

Alginate is an anionic polysaccharide and a linear copolymer including blocks of β-D-mannuronic acid monomers (M) in sequence with α-L-guluronic acid blocks(G) It has low toxicity and gels under gentle conditions. A gel can be easily achieved through ionic bridge formation between G blocks by adding divalent cations [53]. Due to the easy crosslinking, alginate has been widely used in bioprinting application. Boland et al. first reported use of alginate to fabricate 3D structure in 2006 and layer-by-layer structure was achieved [45]. One limitation of using alginate in tissue engineering is that it does not have cell-binding sites, which may be not good for cell adhesion. This limitation could be overcome by mixing with cell responsive molecules such as gelatin.

### 2.3.2 Synthetic hydrogels

#### *2.3.2.1 Poly (ethylene glycol) PEG*

PEG possesses a lot of good properties such as biocompatibility and hydrophilicity and chemical tailorability with modifying with various functional groups [54]. The rheological properties and mechanical properties can be tuned by simply changing the molecular weight of the polymer. According to the degree of polymerization, there are various molecules with different molecular weight including PEG (molecular weight ($M_w$)< 20kDa), PEO ($M_w$>20kDa) or poly(oxyethylene) (any $M_w$). The polymer alone cannot form physical or chemical gel while chemical modification can facilitate the use in bioprinting. Acrylation of PEG can create a photocrosslinkable hydrogel (PEGDA) in which cells can be encapsulated. Though PEG is inert to cell, some bioactive molecules such as cell-adhesion motifs can be encoded into PEG chain, resulting in a bioresponsive environment [54]. Hockaday et al. utilized extrusion-based printer to print a PEGDA-alginate hydrogel where porcine aortic valve interstitial cells were encapsulated to fabricate a mechanically heterogeneous aortic valve structure. The major function of PEGDA in this system is to maintains the shape after photopolymerizing [55].

Table 2 is adapted from ref. [56]. It briefly summarizes the recently used biomaterial for 3D bioprinting. Generally, selecting natural hydrogel for 3D bioprinting can benefit from their ability to mimic human ECM, their congenital bioactivity and easy degradation by body. Despite their advantageous biological properties, natural hydrogels have some drawbacks such as relatively quick degradation time and poor mechanical properties. For synthetic hydrogel, molecular weights and crosslinking densities can be controlled to tune specific mechanical properties. Limitations of selecting synthetic hydrogel for 3D bioprinting include poor biocompatibility and toxic degradation produces. Even so, synthetic hydrogels still attract researchers' interest due to their hydrophilicity and tunable physical properties.

Table 2 Biomaterial for 3D bioprinting [Taken from ref. [56]]

| Material | Modification | Synthetic/ natural | Crosslinking method | Crosslinking speed | Pros | Cons | Common applications |
|---|---|---|---|---|---|---|---|
| Polyethylene glycol (PEG) | PEGDA (Acrylated) | Syn. | Photopolymerization | Minutes | Easy to control mech. properties by changing MW | Not cell-adherent without modification | Cell encapsulation<br>Cell delivery<br>Crosslinker for other polymers |
| PEG | Multi-arm geometries (4-arm, 8-arm pendent chains, *etc.*) | Syn | Photopolymerization | Minutes | Modulation of mech. properties by increasing/decreasing crosslinking density | Not cell-adherent without modification | Cell encapsulation<br>Cell delivery<br>Crosslinker for other polymers |
| Collagen | – | Nat. | Hydrophobic bonding | 0.5–1 h | Naturally cell adherent<br>Major component of native ECM | Slow gelation | Implants<br>Cell encapsulation<br>Substrate coating<br>Dermal substitutes |
| Hyaluronic acid | Thiolated | Nat. | pH-mediated Michael addition | 15–30 min | Commercially available in kit w/gelatin for cell adherence<br>Mech. properties can be modulated by crosslinkers | Generally low mechanical properties | Cell encapsulation<br>Cell delivery<br>Wound healing |
| Hyaluronic acid | Thiolated | Nat. | Photopolyrmerizatiori (thiol-ene) | Seconds | Easily controllable fast gelation | Generally low mechanical properties | Cell delivery<br>Wound healing<br>Bioprinting |
| Hyaluronic acid | Methacrylated | Nat. | Photopolymerization | Minutes | Gelation speed modulated by UV intensity | Generally low mechanical properties | Cell encapsulation<br>Bioprinting |
| Hyaluronic acid | Tyramine | Nat. | Tyramine-$H_2O_2$ | Seconds | Fast gelling | Difficult to control geometry due lo fast gelation | Tissue filler<br>Cell encapsulation |
| Gelatin | – | Nat. | Temp.-based hydrophobic bonding | Minutes–hours | Naturally cell-adherent | Unstable | Cell encapsulation |
| Gelatin | – | Nat. | Glutaraldehyde | Hours | Naturally cell-adherent<br>Stable after crosslinking | Crosslinking must be performed prior to addition of cells | Scaffolds and films |
| Alginate | – | Nat. | $Na^+$ to $Ca^{2+}$ ion exchange | Seconds | Easy to create gel microspheres | Difficult to control geometry due to fast gelation<br>Not cell-adherent without modification | Cell encapsulation in microspheres |
| Fibrin | – | Nat. | Thrombin-fibrinogen | Seconds | Fast gelation<br>Cell adherent | Difficult to control geometry due lo fast gelation | Cell delivery<br>Cell encapsulation |
| Polycaprolactone | – | Syn. | Melt-cure | – | Robust mech. properties | High temps<br>No cell encapsulation | Structural support<br>3-D scaffold fabrication |

## 2.4 Hydrogel Properties in Bioprinting

Desired physicochemical properties are required for a hydrogel under fabrication conditions imparted by different biofabrication instruments. The major physiochemical properties include rheological properties such as shear-thinning and viscosity, and the crosslinking mechanism by which the hydrogel forms a stable structure.

### 2.4.1 Viscosity and shear thinning

Viscosity is a material's resistance to flow upon application of stress. Rheological properties of ink should be characterized for smooth extrusion. The most important part during extrusion is the nozzle tip under high shear rate (~20-200$s^{-1}$) where if the viscosity is too high, the chocking and fracture will be easy to occur [57, 58]. After extruding out of nozzle tip, a high viscosity is required to avoid tension-drive droplet formation [59]. Polymers with shear thinning behavior can facilitate this process. Shear thinning is non-Newtonian behavior of fluids whose viscosity increases with decreasing shear rate (Figure 5). This phenomenon can be explained by that the shear force reorganizes the polymer chains from an entangled conformation to a stretched one, resulting in decreasing viscosity. For non-Newtonian material, the power-law model has been extensively used to describe rheological properties. In this model, the data is matched in Equation 2.1 [60]

$$\eta=\frac{\tau}{\dot{\gamma}}=K(\dot{\gamma})^{n-1} \quad (2.1)$$

Where $\tau$ is the shear stress (Pa), $\eta$ the apparent viscosity (Pa· s), $\dot{\gamma}$ shear rate ($s^{-1}$), n is power law index and K is the consistency index ($Pa\cdot s^n$). K gives an idea of viscosity of the fluid. The increasing of K indicates the increase of viscosity [61]. The flow behavior can be classified into three groups based on the value of n: n>1: shear-thickening behavior; n=1: Newtonian behavior; n<1: shear thinning behavior. The smaller the n value, the more shear thinning is the material [62].

The polymer concentration and molecular weight predominantly determine the viscosity of solution. Table 3 shows some polymers' viscosity and their molecular weight(Adapted from ref. [59]). The printing fidelity can increase with increasing viscosity. Gaetani et al.

utilized different concentrations of alginate for printing including 5%, 7.5% 10% alginate. The structure printed by using 7.5% and 10% alginate could be more defined [10]. Schuuirman et al. reported that 20% GelMA could form droplets at the tip of the needle due to low viscosity at 37 °C, while 2.4% hyaluronic acid (HA) that had high molecular weight was added to allow the formation of filament [24].

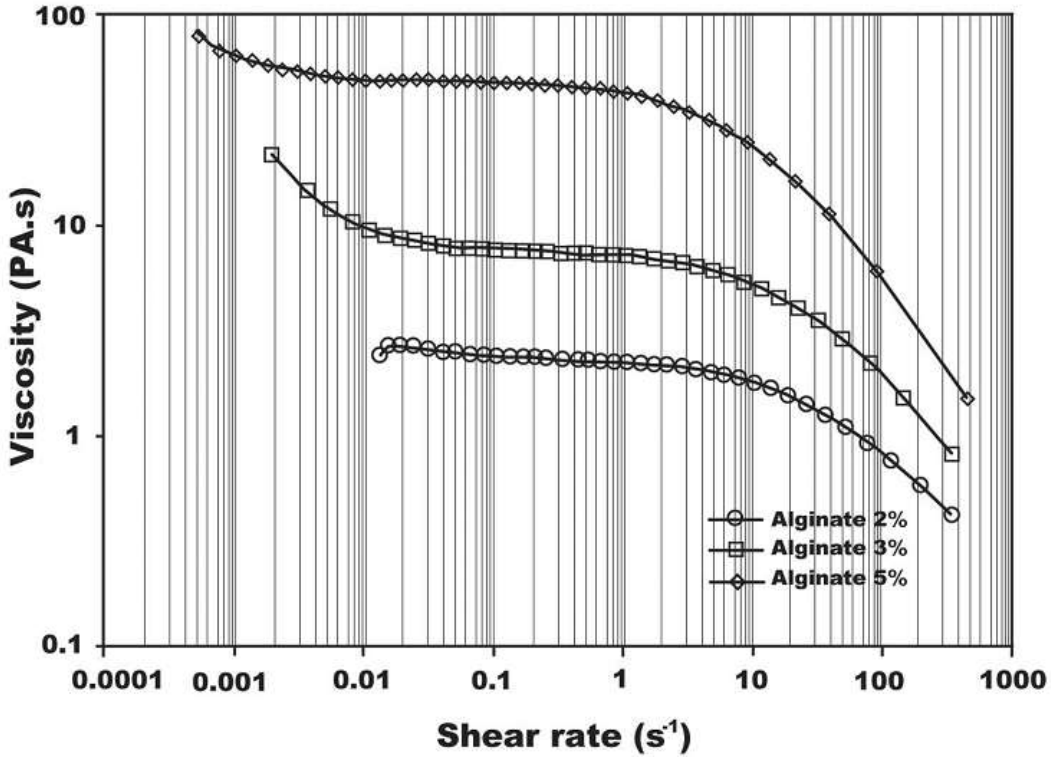


Figure 5. Shear thinning behaviour. [Taken from ref.[63]]

Table 3 viscosities of some polymer solutions in 3D printing. [Taken from ref. [59]]

| polymer | concentration % w/v | viscosity (Pa·s) | shear rate ($s^{-1}$) | molecular weight (kDa) |
|---|---|---|---|---|
| sodium alginate | 2 | 0.9 | 100 | 100–500 (typical) |
| | 3 | 2.0 | | |
| | 5 | 6.4 | | |
| Lutrol F127 | 25 | 0.03 | – | 12 |
| | 30 | 1.5 | | |
| | 35 | 26 600 | | |
| | 40 | >600 000 | | |
| PEG | 10 | 0.008 | 200–1300 | 3.35 |
| | 20 | 0.017 | | |
| Hyaluronic acid | 1.5 | 22 | 1 | 950 |
| Collagen type I | 0.3 | 10 | 0.1–100 | 115 + 230 |

### 2.4.2 Crosslinking mechanism

Crosslinking is necessary to generate 3D network and maintain the final shape of printed constructs. It has been commonly perceived that quick gelation before the spreading and collapse of printed structure would be desirable in some 3D bioprinting application such as extrusion, which can maintain their structural integrity [64]. For example, Melchels et al. reported the improved fidelity of the structure after the incorporation of gellan gum in GelMA to fasten the gelation [65]. The crosslinking method should also be carefully selected since the mechanism may affect cell viability. It is better that crosslinking process is noncytotoxic and the crosslinked hydrogel should be stable at physiologic temperature and pH.

There are various cross-linking mechanisms including temperature-, photo-, enzyme-induced crosslinking. Thermal-induced gelation can produce a temporary shape that can transit from solution to gel at certain temperature. This sol-gel transition temperature is also called the critical solution temperature. There are two types of hydrogel that have an upper critical solution temperature (UCST) or lower critical solution temperature (LCST). For hydrogel with LCST, semisolid gel will form above LCST. On the contrary, hydrogel with UCST can form semisolid gel below UCST. The rate of sol-gel transition depends on

distance from the critical solution temperature [8]. Gelatin is a thermorepsonsive gelation material with UCST around 30 ℃ whose property can be utilized in bioprinting to help maintain the printed constructs [66]. However, the gelatin alone cannot be used in 3D bioprinting as it cannot maintain its shape at physiological temperature that is above its UCST.

A permanent shape is necessary to lower deformation as time goes by. Polymers with chemical gelation can form chemical covalent bonds which can achieve long-time stability. For example, polymers can be grafted with acrylate or methacrylate groups and then be photocrosslinked to form a covalently bonding network. Gelatin is modified with methacrylamide groups to be a photocrosslinkable material Gelatin metahcrylamide (GelMA). The mechanical properties can be tuned by the degree of modification. The combination of thermal and chemical crosslinking can facilitate the bioprinting process. Billiet et al. reported successful printing of GelMA by precise control of the ink and nozzle temperature and constructed interconnect pore network [28] however there was a slight collapse of structure of 10% GelMA due to its slow thermal gelation. Increasing GelMA concentration could fasten the physical gelation but the concern was that the high amount of polymer concentrations may limited cell migration and proliferation.

Enzymatic cross-links are based on enzyme-catalysed covalent bonding. Transglutaminase (EC 2.3.2.13) belongs to the class of transferases. Transglutaminase-induced enzymatic crosslinking can catalyse reaction between γ- carboxamides of glutamine residues and primary amine groups (acceptor of acyl) (Figure 6a) including the amino groups of lysine (Figure 6b). If there is no amine group existing, water can serve as the acyl acceptor (Figure 6c). The reaction can result in change of the physical and chemical properties of substrates, such as viscosity, thermal stability [30].

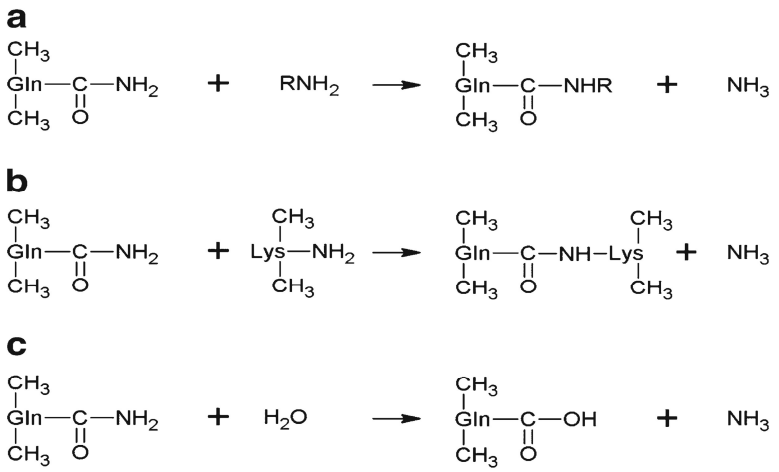


Figure 6. Transglutaminase-induced reaction. (a) acyl transfer between glutamines and primary amine groups (b) acyl transfer reaction between glutamines and lysine (c) hydrolysis of glutamines [Taken from ref. [30]]

MTGase has been widely used to crosslink gelatin for various applications including drug delivery [67], injectable cell delivery gel [68] and scaffold fabrication [69]. The enzyme transglutaminase has been reported to be biocompatible and immunogenic [70]. Recently, MTGase has been used in 3D bioprinting. It was reported that Irvine et al. used gelatin, crosslinked with MTGase to print 3D construct. The chemical gel formed after enzymatic crosslinking could permanently fixed the shape. However, the enzymatic crosslinking was proceeding during printing so the time taken to fabricate the constructs reported which was within the pre-gelation initiation time window was very short: 3 mins for 3% Gelatin/2% PEO with 3 U/mL MTGase and 8 mins for 5% gelatin with 3 U/mL MTGase. The short fabrication time made it difficult to control and could not fabricate large structure [71].

## 2.5 Challenges of hydrogels in 3D Bioprinting

Bioprinting imposes contrasting requirements of hydrogel [59]. Increasing polymer concentration results in a highly viscous hydrogel precursor and a high crosslinking density aids in maintaining the shape, providing good shape fidelity [10, 11]. For cell point of view, cells prefer to encapsulate in an aqueous hydrogel with high water content where a dense polymer network do no limit its spreading, migration and proliferation.

# Chapter 3

# Experimental Methodology

*Experimental methodology is described in this chapter. The experimental design is outlined (Section 3.1), followed by describing the materials (Section 3.2) used in this thesis. Finally, the characterization methods and technologies (Section 3.3-3.7) applied in this research were introduced in detail, including NMR characterization, rheology characterization,3D bioprinting process, cell culture and cell viability staining.*

## 3.1 Experimental design

### 3.1.1 GelMA

GelMA is a gelatin-based hydrogel modified with methacrylamide and a minority of methacrylate groups. GelMA retains biological properties from gelatin containing cell adhesion motifs (arginine-glycine-aspartic acid (RGD) sequences) and target sites for matrix metalloproteinase (MMP) in cell remodeling and degradation [18]. Its photo-crosslinkable property enables quick formation of a covalently crosslinked hydrogel and maintaining the printed construct; and thus become stable under physiological temperature for further 3D cellular culture.

GelMA is an attractive and promising printing material with superior biological properties for 3D bioprinting. However, direct extrusion printing of GelMA still faces some challenges due to its poor rheological properties such as low viscosity and slow gelation. For example, Schuurman et al. has reported that printing GelMA requires relatively high polymer concentration due to its low viscosity at 37 °C [24]. However, a dense hydrogel network is not desired for cell encapsulation with limited cell activities and can limit nutrient and waste transportation and inhibit formation of new ECM and matrix remodelling [72]. Additionally, to improve the printability of GelMA, precise control of the nozzle temperature and cooling down the platform have been conducted to successfully print GelMA but the hardware became important [28]. Moreover, prepolymerizing GelMA is another strategy for direct printing GelMA. Bertassoni et al. has directly printed GelMA with concentrations ranging from 7-15% by prepolymerizing GelMA through photocrosslinking inside a glass capillary [73]. Nevertheless, the limitation associating with this system is that it does not allow for dispensing of continuous fibers as the glass capillary is brittle and easy to break. Therefore, it is imperative to develop a novel strategy that enables direct bioprinting of cell-laden GelMA with a delicate balance between a good structural fidelity and proper cell activities.

### 3.1.2 Enzymatic crosslinked GelMA (MTGase-GelMA) solutions

MTGase induced-crosslinking can catalyze reaction between γ- carboxamides of glutamine residues and primary amine groups (acceptor of acyl) as mentioned in section 2.4.2. Literature has shown that MTGase treatment of gelatin can influence the properties such as increased viscosity [74], thus in the current study, it is intended to alter the rheological properties of GelMA solution through MTGase treatment. The mechanism is shown as below (Figure 7). The resulting solution is named as MTGase-GelMA.

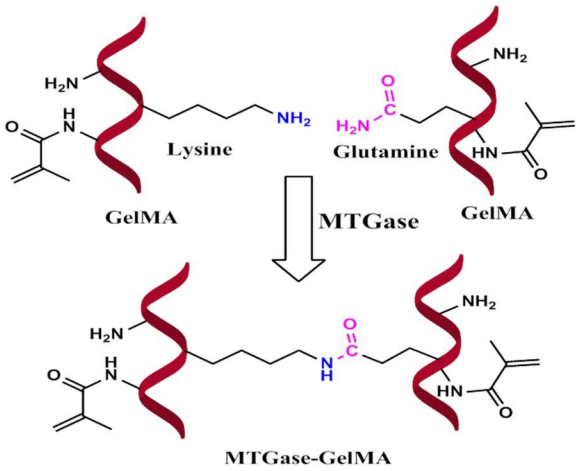


Figure 7. the crosslinking mechanism of MTGase-GelMA hydrogel.

Additionally, to better control the degree of enzyme crosslinking and avoid forming a chemical gel with irreversible shape, thermal inactivation (80 ℃, 10 mins) of MTGase can be conducted to inactivate MTGase.

In our design, the goal is to tailor rheological properties of GelMA and improve its poor rheological properties (such as low viscosity and slow thermal gelation) to develop a novel bioink for bioprinting. So we intend to increase viscosity and induce shear thinning behavior of GelMA by MTGase treatment. Meanwhile, we aim to raise sol-gel transition temperature of GelMA after MTGase treatment. Raised sol-gel transition temperature can fasten the thermal gelation while sol-gel transition temperature above room temperature (25 ℃) could facilitate GelMA processing gel-like character under printing condition as well as a good shape fidelity. However, it is ideal that sol-gel transition temperature is

below 30 ℃ so that the materials are in solution state at 37 ℃, which can ensure providing enough time (10-15 min) to mix with cell and make the solution homogenous. These temperature-dependent physical properties are advantageous to facilitate the cell encapsulating into MTGase-GelMA before printing.

### 3.1.3 Development of bioink based on MTGase-GelMA

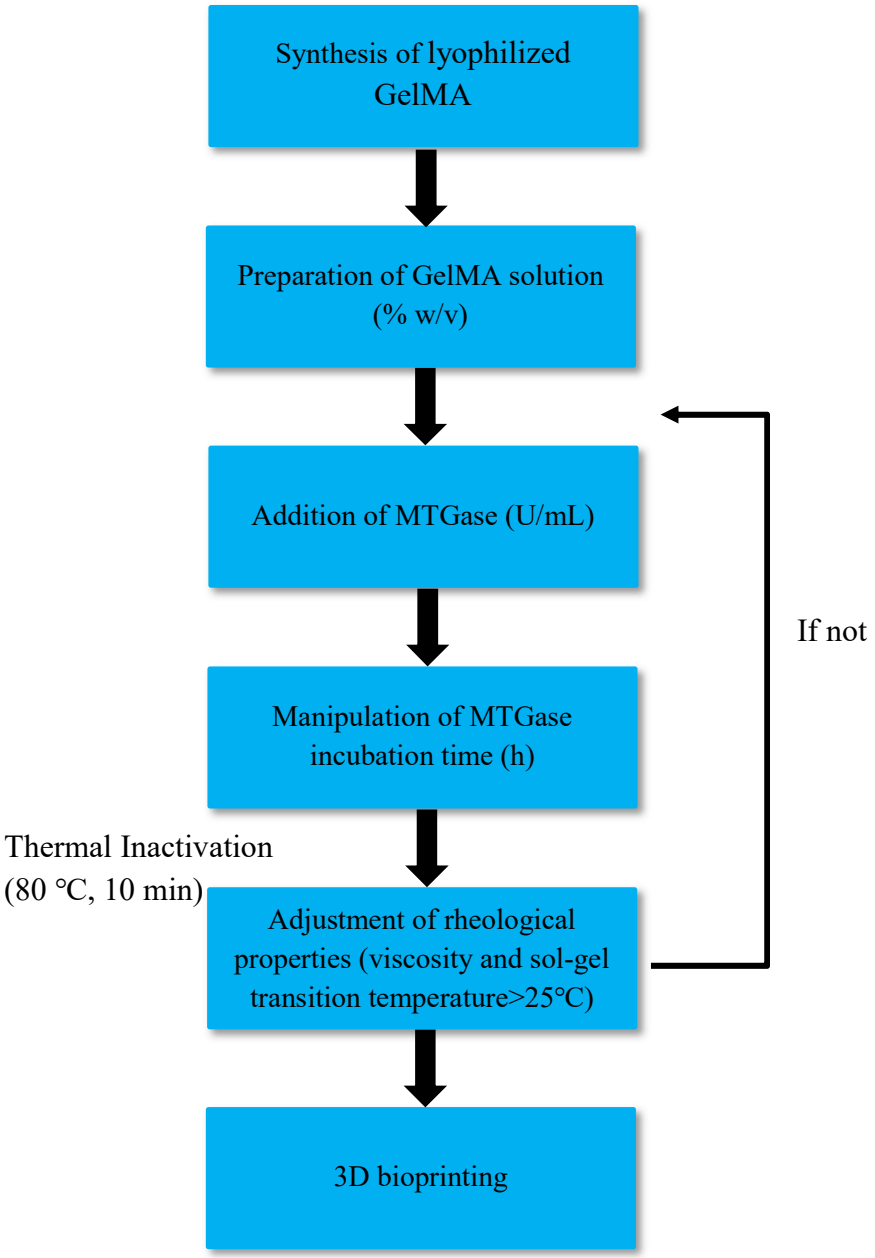


Figure 8. illustration of iteration design.

Due to the variability of starting materials-gelatin (bloom strength; origin), different synthesis methods and the resulting degree of methacryloylation, the rheological properties of GelMA from batch-to-batch may be different [75].To eliminate the batch-to-batch variability and develop bioink based on MTGase-GelMA, an iteration process was designed as below (Figure 8). One set of the iteration process is illustrated from 4.1-4.2;

## 3.2 Materials

Methacrylic anhydride (MAAnh), Irgacure 2959 (I2959), deuterium oxide and gelatin (gel strength~ 175g Bloom, type A from porcine skin) were purchased from Sigma-Aldrich (Singapore). Methacrylic anhydride was a reactant for synthesizing gelatin methacryloyl. I2959 is the most reported photo initiator for GelMA due to its water solubility and relatively low cytotoxicity compared with other photo initiators [76]. The microbial transglutaminase (MTGase) was obtained from Ajinomoto (Japan). The microbial transglutaminase powder with sodium casinate and maltodextrin additives has an enzymatic activity of 100 U/g.

## 3.3 Synthesis of GelMA

Synthesis of GelMA was under optimized condition followed previous work[77]. Briefly, GelMA was prepared by reaction of type A gelatin with methacrylic anhydride as following: 7.95 g of $Na_2CO_3$ and 14.65 g of $NaHCO_3$ were dissolved in 1 L distilled water to produce 0.25 M carbonate-bicarbonate (CB) buffer solution. Following that, 50 g of Gelatin was dissolved into 500 mL of the as-prepared buffer. The pH value of the gelatin solution was gradually adjusted to 9 by adding 5 N NaOH solution in a dropwise manner. MAAnh was added to the solution to achieve an MAAnh : gelatin ratio of 0.05 mL/g. The reaction proceeded at 50 °C for 3 h. 1 N HCl was added and the reaction stopped when the pH value of the solution was adjusted to 7.4. The crude product was filtered and dialyzed to remove any unreacted MAAnh and methacrylic acid by-product. Finally, GelMA was lyophilized to obtain a dried product and stored at -20 °C for future use.

### 3.4 $^{1}$H NMR characterization

The methacryloylation of gelatin was measured by using $^{1}$H NMR spectroscopy. The GelMA solution had a concentration of 50 mg/mL in $D_2O$ and $^{1}$H NMR spectra were repetitively collected for three times. Purely absorptive signals were corrected by phase correction. The areas of the peaks were integrated after baseline correction. The degree of methacryloylation (DM) was defined by Equation 3.1 where the percentage of ε-amino groups of gelatin modified with methacryloyl groups was calculated.

$$DM(\%)=\left(1-\frac{A(\text{Lysine methylene of GelMA})}{A(\text{Lysine metheylene of unmodified gelatin})}\right)\times 100\% \quad (3.1)$$

### 3.4 Preparation of MTGase-GelMA solutions

GelMA solution was prepared by dissolving the lyophilized GelMA at the concentration of 10% (w/v) in phosphate buffered saline (PBS) solution. Different amount of MTGase were separately added to the as-prepared GelMA solutions so that the final concentrations were 1, 3 and 5 U/mL. The incubation temperature was 37 °C. The MTGase was inactivated by heat treatment (80 ℃, 10 min).

### 3.5 Rheological characterization

The rheological properties of the enzymatic crosslinked were tested by a rheometer (MCR 501, Anton Paar Physica, Ostfildern, Germany) with cone-plate geometry. To study the formation of gel network, the time sweep test was performed where storage modulus (G') and loss modulus (G") were monitored as a function of time at a fixed frequency of 1 Hz and strain of 3%. To avoid evaporation of water, the MTGase-GelMA solutions were sealed in the tube and incubated at 37 °C and then sequentially loaded onto the rheometer at an interval of 1 h and tested for 1 min. During testing, measurements were collected every second and the average of the 60 data points represented the average modulus of the sample at different incubation time. The time-dependent viscosity during the proceeding

enzymatic crosslinking was tested at 37 °C under the shear rate of 100 $s^{-1}$, with a similar way of data collection described earlier.

Rheological properties were assessed for printability under printing condition. The solutions were allowed to reach the equilibrium temperature for 2 min prior to performing the experiments. Viscosity was determined under various shear rate from 1 to 1000 $s^{-1}$ under room temperature (25 °C). Temperature sweep was performed from 37 °C to 5 °C at 2 °C/min with frequency of 1 Hz and strain of 3%. To investigate the effect of MTGase treatment on photopolymerization of GelMA, time sweep test was performed at frequency of 1Hz and strain of 3% was performed. Omicure s1000 was equipped with the machine as UV source. Samples containing 0.1% w/v Irgacure 2959 (photo initiator) were placed between the plates and exposed to UV light 365nm at intensity of about 25 $mW/cm^2$. UV exposure times were 5 min for all samples.

## 3.6 3D bioprinting

### 3.6.1 Cell culture

C2C12 was cultured and expanded before bioprinting. The cells were cultured in the cell culture media of Dulbecco's Modified Eagle's Medium (DMEM, Hyclone) supplemented with 10% fetal bovine serum (FBS, Hyclone) and 1% antibiotic-antimycotic (ABAM, Life Technologies), in a humidified atmosphere with 5% $CO_2$ at 37 °C.

### 3.6.2 Bioprinting

In this study, MTGase-GelMA solution was bioprinted by using the RegenHU bioprinter. The syringes, nozzles, and pyrex bottles were autoclaved to avoid contamination. MTGase-GelMA solutions containing 0.1% Irgacure 2959 were sterile-filtered through a 0.2 μm syringe filter under sterile condition. The cell suspension was added to MTGase-GelMA solution, resulting in a final cell concentration of ~$6 \times 10^5$ cells/mL, which was used for 3D bioprinting of the 3D grid pattern with dimension of 1.4 cm × 1.4 cm with line spacing

of 2 mm. The nozzle size is 27G straight nozzle (210 μm). Printing pressure is around 1-2 bar.

### 3.7 Cell viability

Cell viability of C2C12 in the cell-laden printed scaffolds were measured using live/dead assay (Molecular Probes) at 0, 3 and 7 day time point. During culturing, the cell culture medium was changed every 2 days. Fluorescence microscopy (Zeiss Axio Vert. A1) was utilized to image the live/dead staining of cells.

# Chapter 4

## Microbial transglutaminase-induced crosslinking of gelatin methacryloyl to tailor rheological properties for bioprinting

*This chapter focus on the effect of MTGase-induced crosslinking on rheological properties, printability and cell viability of GelMA. GelMA was mixed with different MTGase concentration. Then, the rheological properties of GelMA were examined with different MTGase concentration at different incubation time. Based on rheological study, an optimized mixture was selected for 3D bioprinting. A cell-laden structure was constructed followed by cell viability study.*

### 4.1 Methacryloylation of gelatin

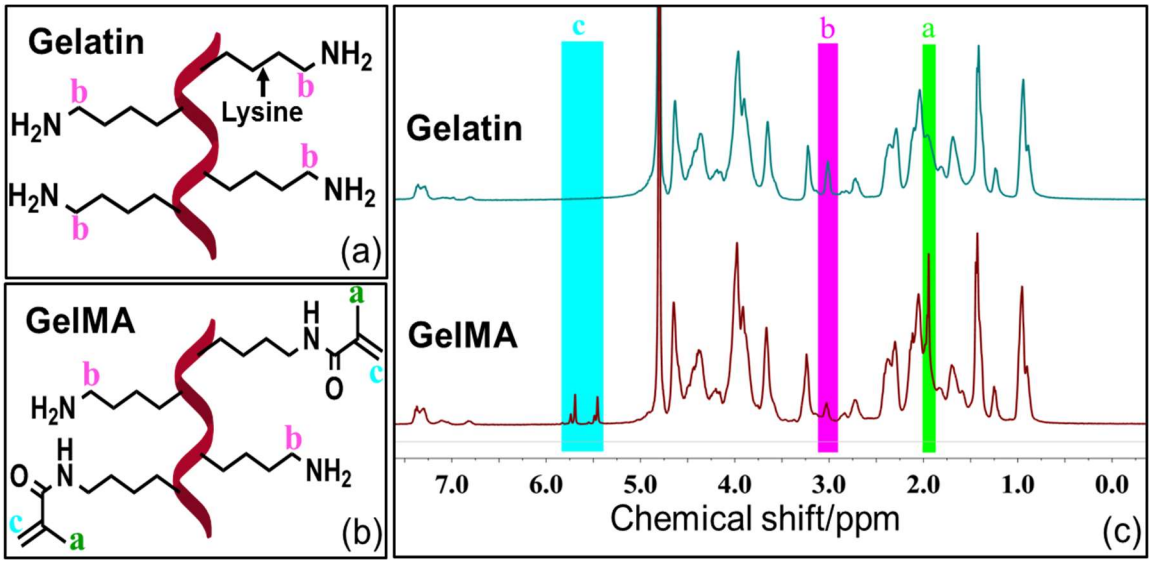


Figure 9. The chemical structures of (a) unmodified gelatin and (b) GelMA, and (c) their respective 1H-NMR spectra. Green "a" and blue "c" represent the signals of the methyl group and acrylic protons of the grafted methacrylic group respectively, and pink "b" indicates the signal of lysine methylene.

The chemical structures of unmodified gelatin and GelMA are shown in Figure 9 a-b. Compared with the spectrum of unmodified gelatin, GelMA sample formed new functional groups marked as green "a" and blue "c" in Fig. 1b, which can be confirmed by the $^{1}$H NMR spectra (Figure 9 c). The peaks at around chemical shifts (δ) of 5.3 and 5.6 ppm could be assigned to the acrylic protons (2H) of the grafted methacryloyl group, and another peak at $\delta = 1.9$ ppm could be attributed to the methyl group (3H) of the grafted methacryloyl group. Meanwhile, there was a decrease of the intensity at $2.9 \leq \delta \leq 3.1$ ppm, which was assigned to the lysine methylene (2H) marked as pink "b". As lysine is the reaction site, this trend could be used to quantify DM yielding around 50%. The remaining lysine groups could be utilized for enzymatic crosslinking as it is an acyl acceptor.

## 4.2 Rheological characterization

### 4.2.1 Gelling period of GelMA incubated with MTGase

The mechanism of enzymatic crosslinking is that MTGase catalyses the inter- and intra-molecular bonds formation between the γ-carboxamides of glutamine residues and ε-primary amino of lysine residues in chains of GelMA as mentioned in 3.1.2. The growth of a connected structure will eventually lead to formation of a chemical gel.

To determine that the reaction took place, a time sweep test was performed at the incubation temperature (37 °C). The effect of the MTGase concentration on the gel formation of 10% GelMA was examined. There were two moduli generated from these experiments: G' representing the deformation energy stored, and G" being the energy dissipated during shear. They are sensitive to molecular structure evolution, especially the formation of network.

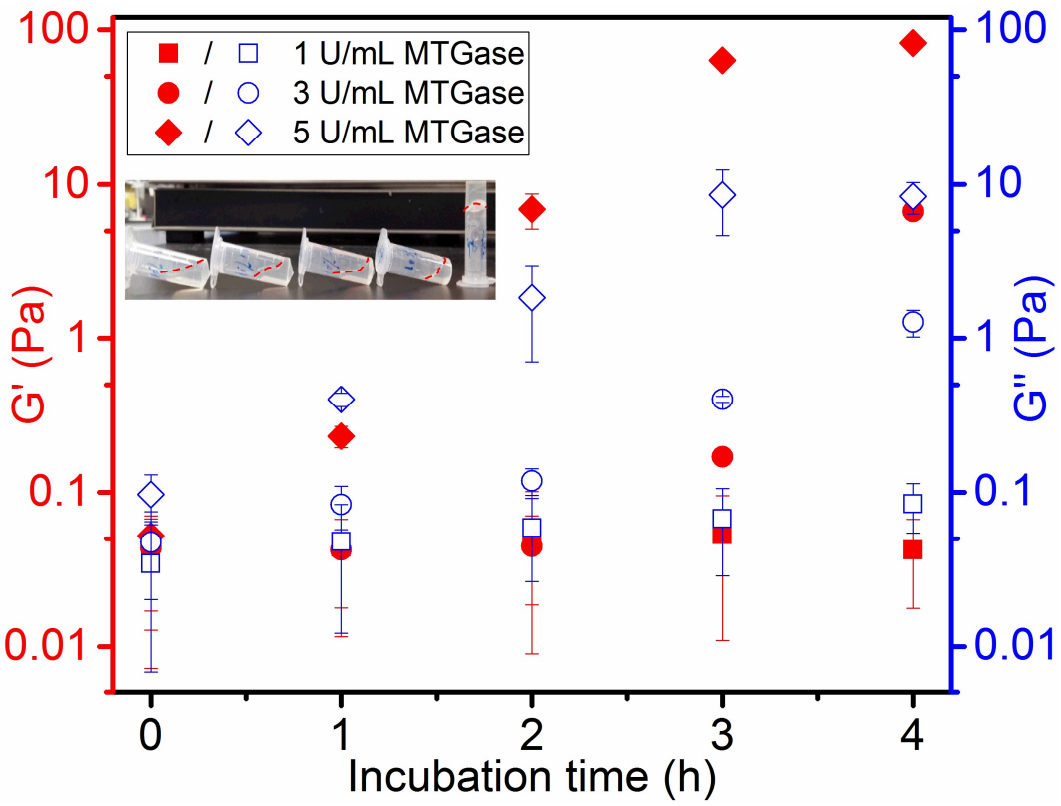


Figure 10. Effect of the MTGase concentration on the gelling period of 10% GelMA solutions at incubation temperature (37 °C). The inset photo shows representative images of transition from a liquid to a chemical gel of 10% GelMA treated with 3 U/mL MTGase at 37°C.

Figure 10 shows that at the beginning, the GelMA solution with MTGase behaves liquid-like where G" is higher than G'. When gelation takes place, there is a crossover of G' and G" (whereby the value of G' is higher) which could be seen for the 10% GelMA incubated with 5 U/mL MTGase. The effect of the concentration of MTGase on the gelling period was summarized in Table 4. There was no gel formation observed for GelMA solution containing 1 U/mL MTGase within 4 h. Above 1 U/mL MTGase, gelling periods were detected when the MTGase concentration was increased: 3-4 h for 3 U/mL MTGase and 1-2 h for 5 U/mL MTGase. Additionally, the gelling period of hydrogels was confirmed by the tube inversion method (Figure 10 inset). Those results reveal that MTGase does exhibit a crosslinking action; the gelling times for the MTGase-GelMA hydrogels are shortened by raising the MTGase concentration due to the enhanced catalytic activity.

Table 4 Gelling period of enzyme-catalyzed MTGase-GelMA with various concentrations of MTGase at 37 °C with a fixed GelMA concentration of 10% (w/v).

| MTGase Concentration (U/mL) | Gelling period (within 4 hours) |
|---|---|
| 1 | - |
| 3 | 3-4 h |
| 5 | 1-2 h |

It has been reported that MTGase catalysed the conversion of gelatin solutions into hydrogels, and gelling times depended on the type and concentration of gelatin [78]. Type A gelatin was selected in the study because Type A gelatin prepared by acid treatment is more effective for enzymatic crosslinking than Type B gelatin prepared by base treatment as base treatment can hydrolyze the amide groups of glutamine residues and suppress enzymatic crosslinking.

### 4.2.2 Viscosity during incubation with MTGase

Viscosity is an important property which affects extrusion process in 3D bioprinting [6]. GelMA has low viscosity, which can inhibit its application in 3D bioprinting [24]. Literature has shown that the viscosity of gelatin solution increased after transglutaminase induced-enzymatic crosslinking [74], so for the current study, it is intended to alter the viscosity of 10% GelMA solution with MTGase treatment, and thus the viscosities of 10% GelMA solutions incubated with different concentrations of MTGase at 37 °C were investigated under the shear rate of 100 $s^{-1}$ that could be the shear rate of materials experienced in the needle tip [57, 79].

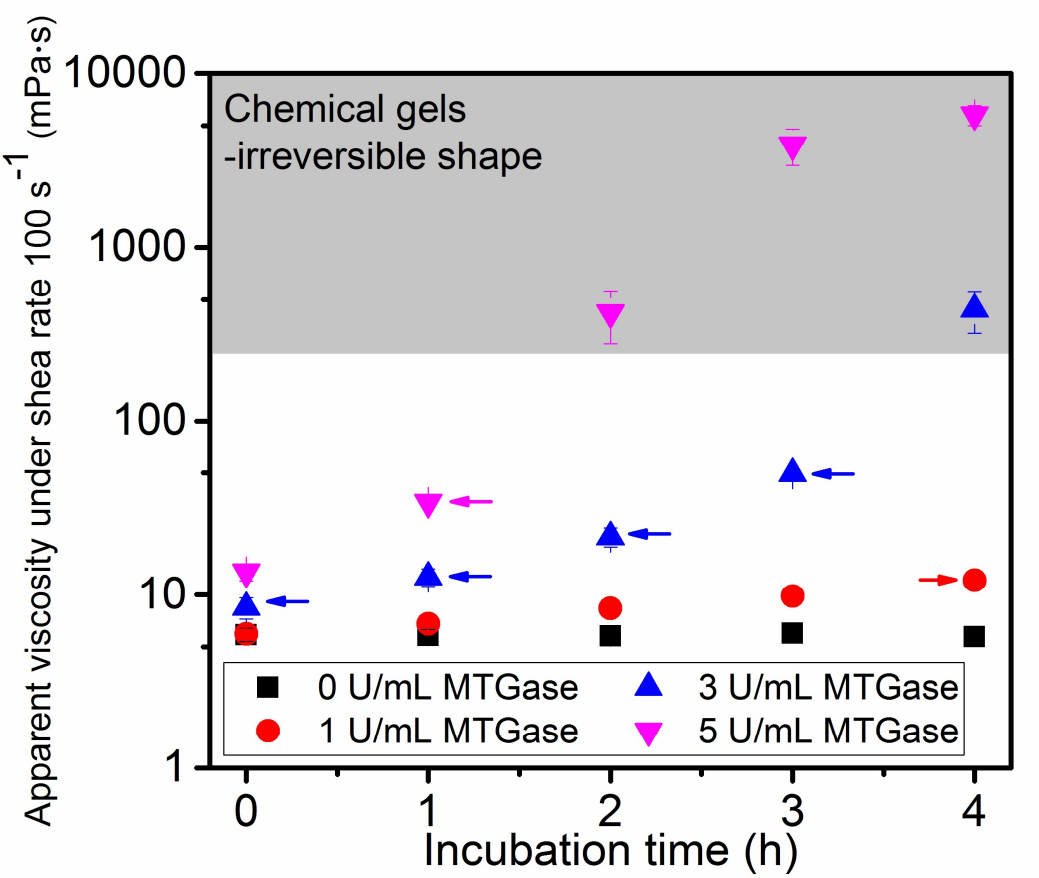


Figure 11. The time-dependent apparent viscosity of 10% GelMA solution incubated with different concentration of MTGase at 37 °C under the shear rate of 100 $s^{-1}$. Arrow marked points were selected and thermal inactivated for further rheological assessment under printing condition.

As shown in Figure 11, the addition of MTGase resulted in a net increase in apparent viscosity during incubation with MTGase at 37 °C due to the polymerization. The rate of apparent viscosity increment was higher by increasing the concentration of MTGase. At the concentration of 1 U/mL, no distinct viscosity increase was observed over 4 h while there was a large increase in viscosity for solutions containing 3 U/mL and 5 U/mL MTGase between 3-4 h and 1-2 h, which could be explained by the formation of a chemical gel as previously mentioned. The addition of MTGase enzyme catalyses the covalent crosslinking action in gelatin, resulting in increased molecular weight and crosslinking degree [80], most likely contributing to higher viscosity when added to GelMA. The resulting increased viscosity could aid in filament deposition however increasing viscosity (Figure 11) may result in inconsistent resolution

and nozzle clogging. Thus, to better control the crosslinking, thermal treatment of the solutions (80 °C, 10 min) was conducted to inactivate MTGase so that the formation of cross-links could be stopped.

For biofabrication application, the apparent viscosity at the shear rate of 100 $s^{-1}$ as shown by the grey shades (Figure 11) would not be considered, because it indicates that chemical gels would have been formed and therefore the shapes were irreversibly fixed and not easy for handling and cell encapsulation. The representative points outside the shaded region were selected and the solutions were thermally treated to inactivate MTGase for further printability assessment under printing condition. The points were labelled shown in the Table 5 and divided into two groups: 0T, 1T4h, 3T3h, 5T1h are 10% GelMA solutions treated with the different concentrations of MTGase, which have the highest viscosity under each concentration before they become chemical gels. 3T0h, 3T1h, 3T2h, 3T3h are 10% GelMA solutions treated with 3 U/mL MTGase over different incubation durations.

Table 5 Labels of MTGase-GelMA solutions

| Group 1 | | | Group 2 | | |
|---|---|---|---|---|---|
| Label | Concentration of MTGase (U/mL) | Incubation time (h) | Label | Concentration of MTGase (U/mL) | Incubation time (h) |
| 0T | 0 | - | 3T0h | 3 | 0 |
| 1T4h | 1 | 4 | 3T1h | 3 | 1 |
| 3T3h | 3 | 3 | 3T2h | 3 | 2 |
| 5T1h | 5 | 1 | 3T3h | 3 | 3 |

### 4.2.3 Rheological assessment for printability under printing condition

To examine the effect of different shear rates on viscosity of the hydrogels during printing process, the rheological properties of the representative points aforementioned were studied at 25 °C under shear rate of 1-1000 $s^{-1}$. The solutions were load at rheometer and were allowed to reach the equilibrium temperature for 2 min prior to performing the experiments. The resulting rheological data were plotted in Figure 12 and matched to the power law model (as mentioned in Section 2.4.1). Lower n represents more shear thinning in the materials, while higher K means the materials are much thicker.

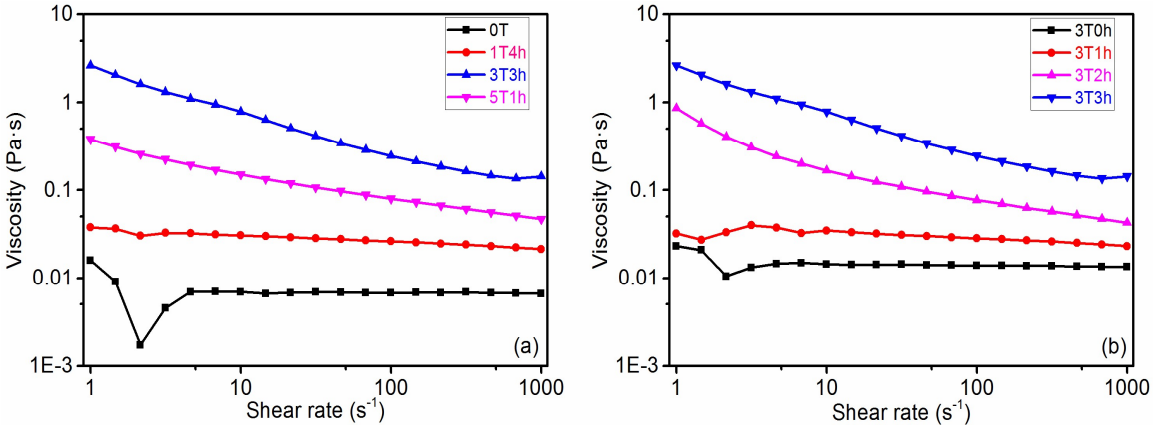


Figure 12. Flow behaviour of 10% GelMA without/with MTGase treatment under room temperature (25 °C) (a) Group 1; (b) Group 2.

Table 6 Power law index n and consistency index K

| Group 1 | | | Group 2 | | |
|---|---|---|---|---|---|
| Label | Power law index n | Consistency index K | Label | Power law index n | Consistency index K |
| 0T | 0.999 ± 0.016 | 0.007 ± 0.001 | 3T0h | 0.968 ± 0.019 | 0.016 ± 0.030 |
| 1T4h | 0.894 ± 0.041 | 0.050 ± 0.016 | 3T1h | 0.929 ± 0.017 | 0.243 ± 0.011 |
| 3T3h | 0.542 ± 0.011 | 2.224 ± 0.530 | 3T2h | 0.646 ± 0.044 | 0.439 ± 0.170 |
| 5T1h | 0.683 ± 0.025 | 0.386 ± 0.079 | 3T3h | 0.542 ± 0.011 | 2.224 ± 0.530 |

From the data listed in Table 6 Power law index n and consistency index K, all samples exhibited shear thinning behaviour ($n < 1$). From Table 6 Power law index n and consistency index K Group 1, it is obvious that sample 3T3h has the lowest n and the highest K; as compared to 10 % GelMA ($n = 0.99$), shear thinning is greatly enhanced for 3T3h ($n = 0.542$). Table 6 Power law index n and consistency index K Group 2 shows that as incubation time lengthens, n is decreased, and K is increased; most likely, this is contributed by the increased molecular weight and viscosity.

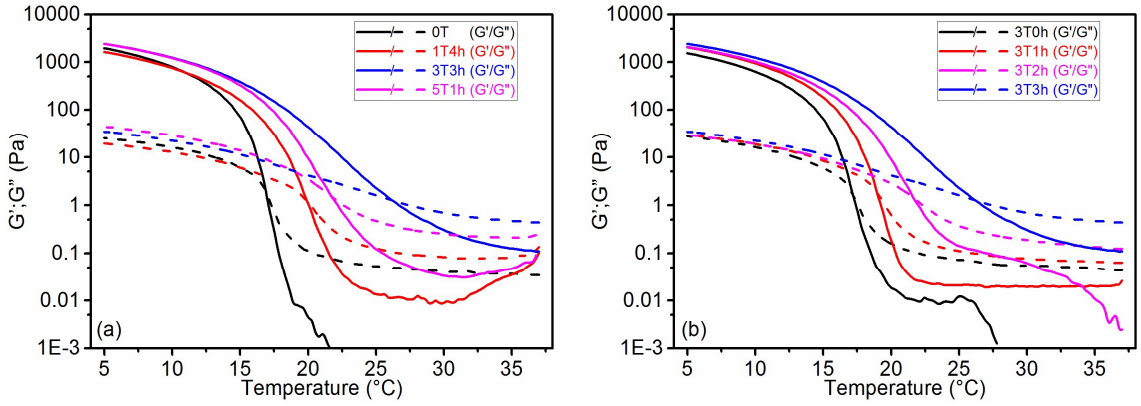


Figure 13. Temperature sweep measurements of 10% GelMA without/with MTGase treatment (a) Group1; (b) Group 2.

It is quite important to investigate the effect of MTGase treatment on the thermal behaviour of GelMA as it is a thermo-sensitive material. To examine the influence, temperature sweep test was performed by cooling samples from 37 °C to 5 °C at 2 °C/min. At 37 °C, the materials show liquid behaviour where G" are higher than storage modulus G'. Upon cooling, G' and G" increase and a crossover occurs (Figure 13). The crossover temperature is assigned as the sol-gel transition temperature (gel point), and it suggests the transition from a solution state to a gel state.

Table 7 Sol-gel transition temperature

| Group 1 | | Group 2 | |
|---|---|---|---|
| Labels | Sol-gel transition temperature (°C) | Labels | Sol-gel transition temperature (°C) |
| 0T | 16.4 ± 0.4 | 3T0h | 17.1 ± 0.2 |
| 1T4h | 20.2 ± 0.4 | 3T1h | 19.2 ± 0.5 |
| 3T3h | 26.0 ± 0.3 | 3T2h | 21.7 ± 0.5 |
| 5T1h | 21.9 ± 0.3 | 3T3h | 26.0 ± 0.3 |

In Group 1, 3T3h has the highest sol-gel transition temperature. From data shown in Group 2 (Table 7), the sol-gel transition temperature increases from 17.1 ± 0.2 °C (3T0h) to 26.0 ± 0.3 °C (3T3h), this implies that extending incubation time could increase the sol-gel transition temperature (Table 7), which can be attributed to the covalent crosslinking action triggered by MTGase, thus leading to a tight network facilitating chain entanglement. It was reported that when the printing temperature was above gelation temperature, the

solution would exhibit liquid behaviour and the viscosity was low, thus being unsuitable for extrusion-based 3D printing studies [81-83]. Except 3T3h, other samples were in sol state with low viscosity at room temperature (25 °C) as their sol-gel transition temperature were below room temperature, hence it would be difficult to achieve good shape fidelity. Considering good shear thinning behaviour, high viscosity and sol-gel transition temperature (above room temperature) simultaneously, 3T3h would be selected for deeper study to check the difference between GelMA treated with and without MTGase.

Check with three different batches of GelMA fabricated in this project, we found that optimized incubation time of MTGase treatment (3 U/mL) was various from 2 to 3 hours with sol gel transition temperature (SG) around 25 ℃ due to the material batch-to-batch dissimilarity. From this point onwards, the 10% GelMA-3U/ml MTGase treated for 2-3 hours is named “SG25 bioink”.

### 4.3 Photopolymerization

While sufficient viscosity is required for printability, further gelation is necessary for handling and maintaining the final shape and thus ensure a prolonged cell culture as well as structural stability under body temperature (37 °C). Thus, time-sweep test for photo crosslinking performed on rheometer was conducted to study the effect of MTGase treatment on photopolymerization of GelMA at 37 °C. The UV light was switched on at 60 s. Figure 14 depicted gelation kinetics of 10% GelMA without/with MTGase treatment; a discernible increase can be observed in G’ indicating the formation of gel network. It seems that the thermal treatment of the materials did not affect the photopolymerization of GelMA. At t = 360 s, the storage modulus of hydrogel (pre-treated with MTGase— “SG25 bioink”) formed after photo crosslinking is higher than that without MTGase treatment. Besides, from the gelation curve of “SG25 bioink” (blue curve), it shows that after 300 s of photo crosslinking, the storage modulus of the hydrogel is much higher than that of solution treated solely with enzymatic crosslinking. This means that photo crosslinking is the dominant mechanism amongst the two; and thus the mechanical properties of the hydrogels can be tuned by photo crosslink in the future.

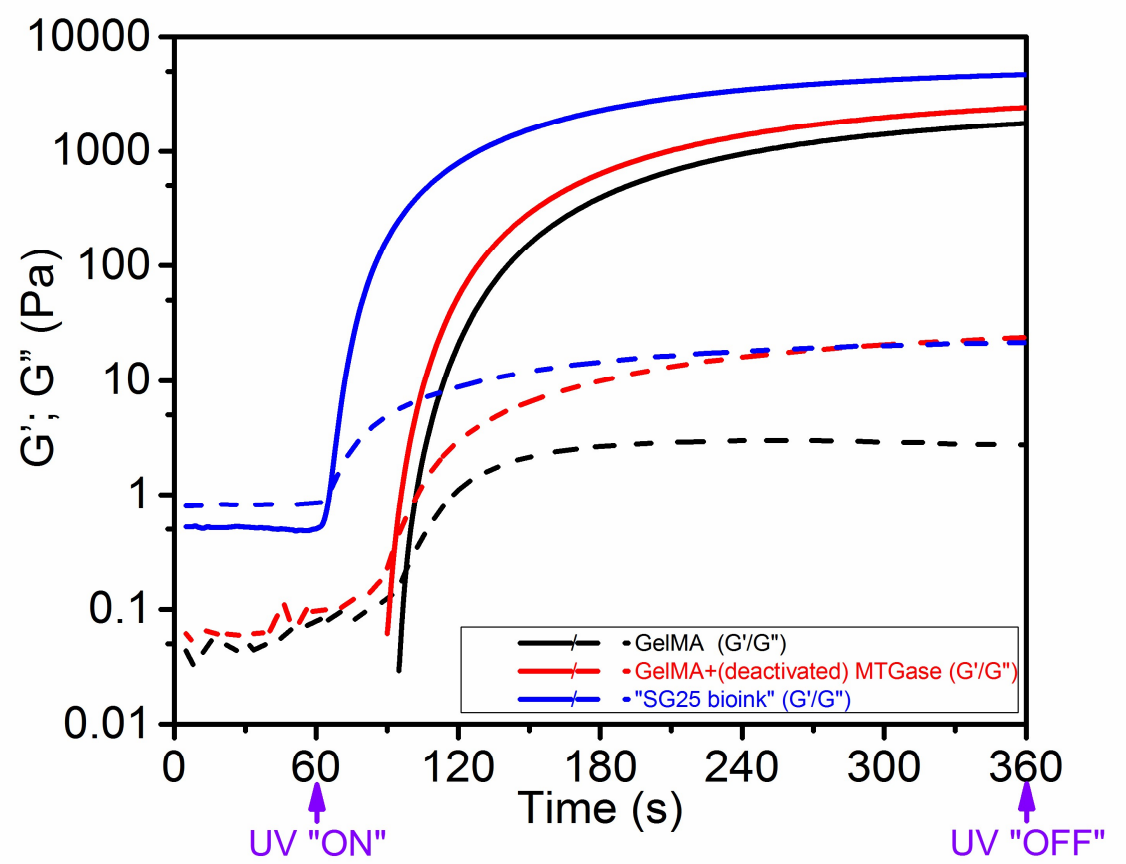


Figure 14. The gelation kinetics of 10% GelMA without/with MTGase treatment at 37 °C.

### 4.4 3D printing

After the materials were developed, printability was investigated as a proof of concept. The printing was conducted at room temperature (25-26 °C). The solutions were kept at room temperature for around 10-20 min and then the printing was conducted. From the picture shown in Figure 15 a, a fine structure could not be achieved with GelMA and GelMA+(deactivated) MTGase. With increasing feed rate, the grid structure gradually became more defined (Figure 15 a) but was still not able to support layer-by-layer stacking due to low viscosity. However, “SG25 bioink” with low feed rate (500 mm/ min) under printing pressure around 1-2 bar could form 5 layers stacking structure. This phenomenon could be due to the increase of solution viscosity after MTGase treatment; the sol-gel transition temperature of “SG25 bioink” is also raised above room temperature (25 °C).

This in turn enables "SG25 bioink" to exhibit gel-like characteristics under printing temperature, thus avoiding ink from bleeding. However, we found that "SG25 bioink" would still not be able to achieve a 10 layers structure with a single print. Thus, in the future we will photocrosslink every 5 layers with a UV pen.

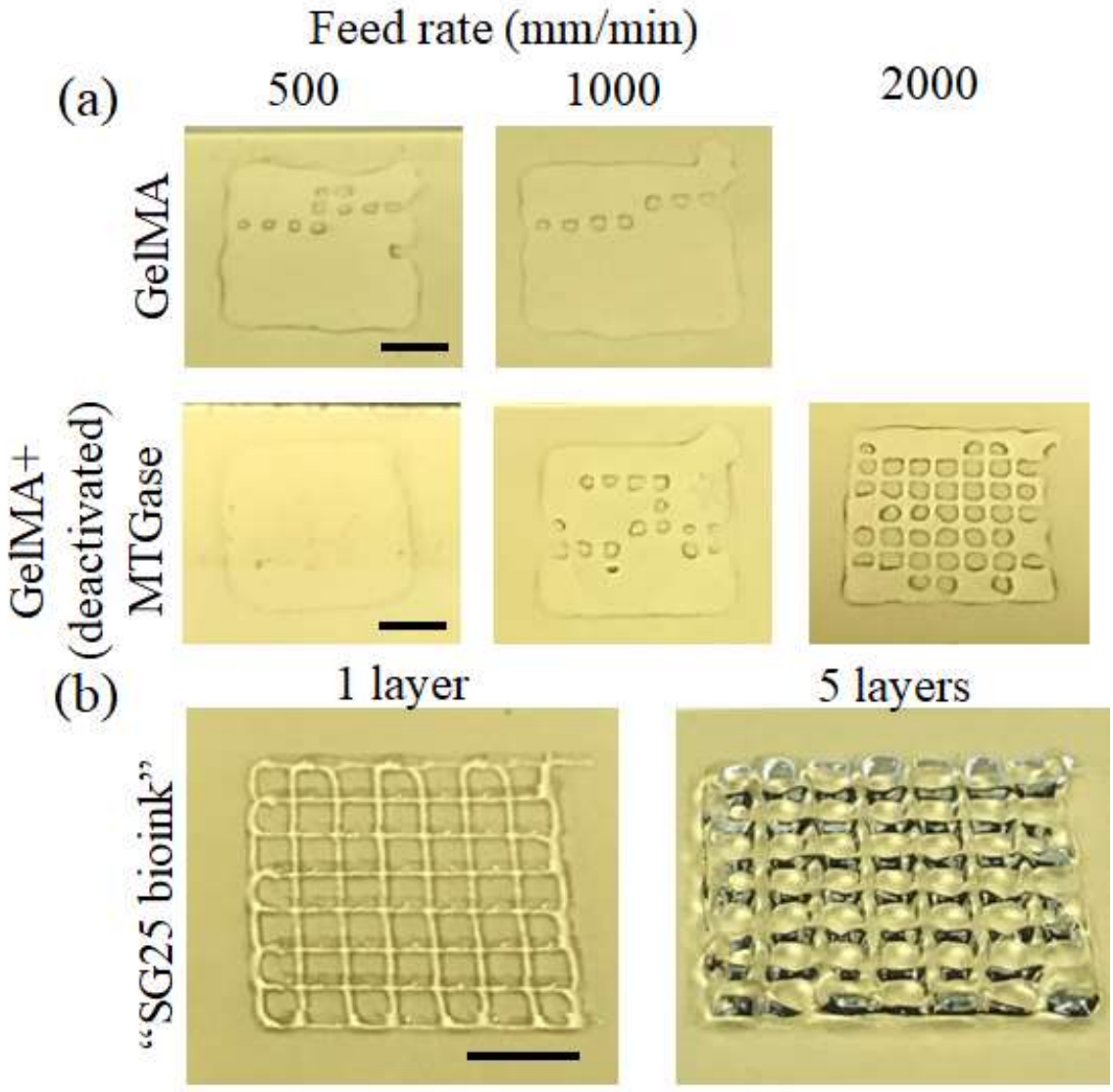


Figure 15.Pictures of 3D grid printing (a) GelMA and GelMA+(deactivated) MTGase under different feed rate (b) "SG25 bioink" under feed rate 500 mm/min (Scale bar=0.5cm).

## 4.5 3D bioprinting

### 4.5.1 Printability of cell-laden "SG25 bioink"

The previous result (Section 4.4) has been proven that "SG25 bioink" was capable to create a 3D structure in bioprinting. As such, it is of interest to investigate the influence of printing process on cell viability and the biocompatibility of "SG25 bioink". Thus, we tested the ability of SG25 bioink to create homogenous cell-laden hydrogel constructs. Further gelation is necessary for handling and maintaining the final shape and thus ensure a prolonged cell culture as well as structural stability under body temperature (37 °C). As mentioned in section 4.4, the structure would be photo crosslinked every 5 layers by using UV pen at feed rate 100 mm/min. From picture shown in Figure 16, we could see that 5 layers and 10 layers could be well constructed. From Figure 17 a, the width of the filament was measured at value of ~ 580 µm. From optical microscope images shown in Figure 17 b, the pore structure appears to be of a square shape, which means that the printed shape could be well maintained.

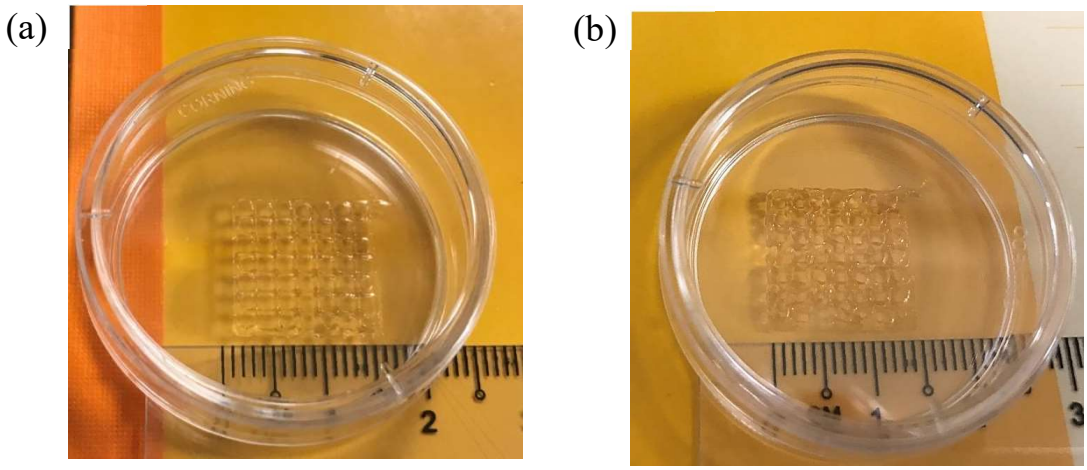


Figure 16. 3D grid structure with cell-laden "SG25 bioink" (a) 5 layers and UV (b) 10 layers. Every 5 layers then UV.

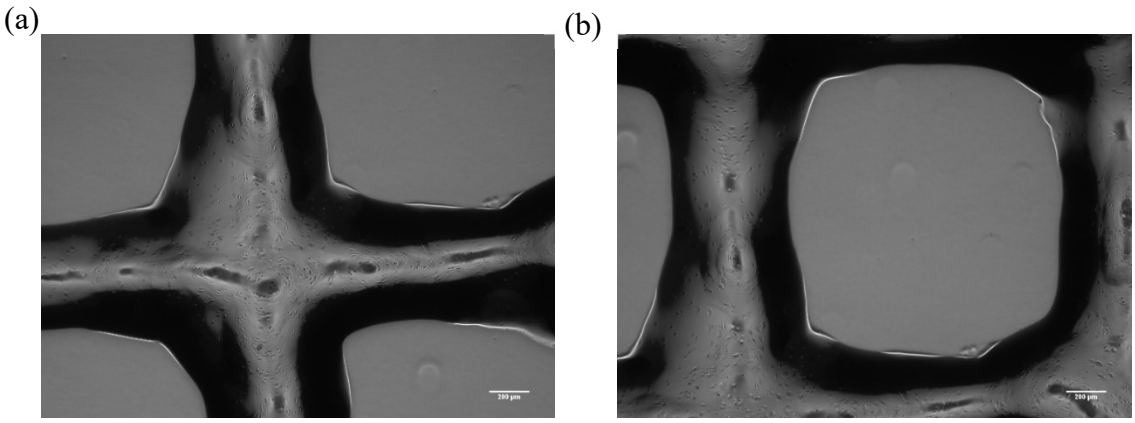


Figure 17. Optical microscope images of five layers constructs. (a) cross-over structure (b) pore structure. Scale bar=200 μm.

### 4.5.2 Cell viability assessment

Stress associated with the printing process has been cited as a common problem that may impact cell viability [73]. To determine the effect of our bioprinting process on the health of cells encapsulated in "SG25 bioink", cell viability of the bioprinted "SG25 bioink" was examined right after printing. (shown in Figure 18 a). The cells used here are C2C12 cells. High cell viability (98.3 ± 1.3%) (Figure 18 a) shows that the printing process using SG25 bioink was not harmful to the cells. Prolonged cell culture (Day 3 and Day 7) showed that cells exhibited elongated morphology compared with that in Day 0 (rounded shape). Cell-cell contact networks were formed after 3-day culture which proves that "SG25 bioink" is biocompatible. It is observed that at Day 7, more cells moved to the edge of the filament which may due to the nutrient gradient effect. Some possible solutions to minimize this effect would be to lower the concentration of initial GelMA to facilitate the media penetration or to have thinner struts.

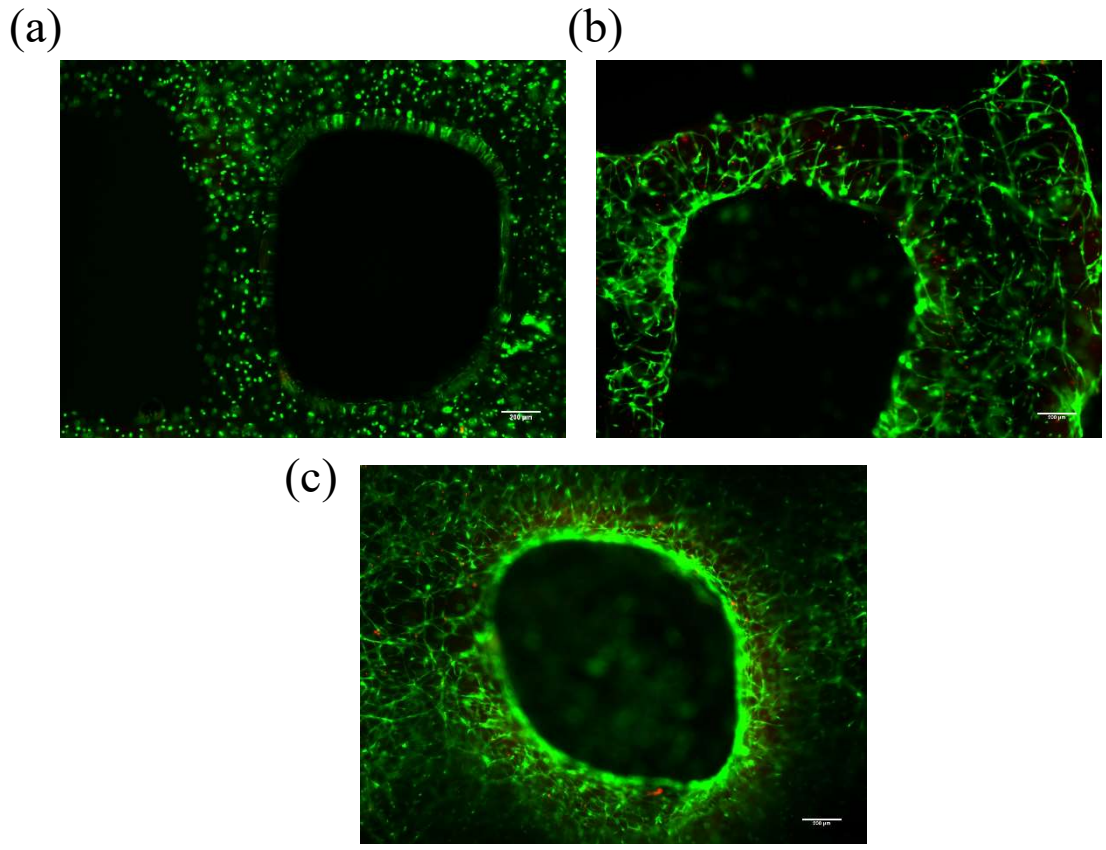


Figure 18. Cell viability of bioprinted "SG25 bioink" (a) Day 0 (b) Day 3 (c) Day 7; C2C12 encapsulated in SG25 bioink were stained with calcein-AM (green)/ethidium homodimer(red) LIVE/DEAD assay (Scale bar =200 µm).

In this thesis, we present a study of modifying a widely used hydrogel, namely gelatin methacryloyl, for applications in 3D printing. GelMA based hydrogels have recently received great interest in 3D printing due to its superior biological properties containing arginine-glycine-aspartic acid (RGD) sequences for cell adhesion and target sequences of matrix metalloproteinase (MMP) for cell remodeling and degradation [18]. Although this has allowed achieving some remarkable successes, there are still some challenges remaining for direct extrusion of GelMA. Researchers have established a variety of strategies including increasing the polymer concentration or combining with other polymers for suitable rheological properties and mechanical properties to improve the printability of GelMA, yet these strategies have limitations. For instance, Schuurman et al. has reported that a relatively high polymer concentration is required to print GelMA due

to its low viscosity at 37 °C [24]. The addition of hyaluronic acid can result in an increment in GelMA's viscosity and thus aid in filament deposition. However, a dense hydrogel network is not desired for cell encapsulation where it can limit nutrient and waste transportation and inhibit network remodeling and formation of new ECM [72]. On the other hand, GelMA has been successfully printed through precise temperature control of the nozzle associated with cooling down the platform but such process requires relatively complex machine [28]. Prepolymerizing GelMA is another strategy for direct printing GelMA. Bertassoni et al. has directly printed GelMA with concentrations ranging from 7-15% by prepolymerizing GelMA through photo crosslinking inside a glass capillary [73]. Nevertheless, the limitation associated with this system is that it does not allow for dispensing of continuous fibers as the glass capillary is very brittle and a careful handling is required to avoid any breakage. In addition, the rapid photo crosslinking is not easy to control.

In conclusion, even though GelMA material has superior biocompatibility, using it as a bioink for 3D printing remains a challenge. The strategies attempted are not ideal as clearly elaborated above. In this work, a new strategy is developed to improve the ability of direct printing 3D cell-laden GelMA constructs by employing a simple and controllable method to prepolymerize GelMA and thus providing a new bioink formulation with benefit of biocompatibility, shear-thinning capability, tunable rheological properties and sequential cross-linking ability towards long-term stable constructs. Such new bioink formulation ("SG25 bioink") was developed by optimizing its rheological properties. After that, cell-laden construct was fabricated.

# Chapter 5

# Conclusion and Future Works

*In this chapter, Section 5.1 summarizes the work conducted for the objective and the overall results and discussion on how the objective were achieved. These results give important hints on the future development of novel bioink for 3D bioprinting. As following, by incorporating the results obtained and literature review, the future research directions have been proposed in Section 5.2. In the future work, it is of interest to explore the concentration and DM of initial GelMA to develop versatile bioink.*

## 5.1 Conclusions

MTGase did catalyse the bond formation in GelMA. The rheological properties of GelMA solution could be tailored by manipulating the enzyme concentration and incubation time so that there was no need to change the polymer concentrations. The printability of GelMA was improved by MTGase treatment. Under the printing condition, the viscosity of GelMA solution after treating with MTGase in low shear rate was around an order of magnitude higher than the value at the high shear rate. The shear-thinning behaviour was apparent, with a flow index of 0.542. Meanwhile, MTGase treatment raised sol-gel temperature of GelMA which could faster physical crosslinking and aid in GelMA exhibited a gel-like character under printing condition and resulting in a good shape fidelity. The fast photo crosslinking could aid in maintaining the final structure shape. The photo crosslink in such dual crosslinks could be dominant; and thus the mechanical properties of the hydrogels can be tuned by photo crosslink in the future. The optimized bioink ("SG25 bioink") was utilized to fabricate a 3D cell-laden structure. High cell viability after printing validated that the printing process did not affect the health of cells. Cells encapsulated in the structure became elongated after long-term culture (3 days and 7 days), which proved the biocompatibility of the novel bioink. According to these results, the treatment of MTGase on GelMA could be a practical method to improve GelMA's printability in 3D bioprinting.

## 5.2 Recommendations for Future Work

From the cell study work mentioned in section 4.5.2, some cells moved to the edge of filaments after 7 days culturing, and this may due to nutrient gradient along the filaments where nutrient is present in the highest concentration at the periphery. In the future, we can try to lower the concentration of initial GelMA to facilitate the media penetration.

It was reported that chemical crosslinking could improve the printability of gelatin [84]. Alexandra et al. utilized (polyethylene glycol X) PEGX (X in PEG=succinimidyl valerate) to partially crosslink gelatin and thus made gelatin printable. They controlled the crosslinking degree by small additions of PEGX so that the material could exhibit soft gel,

which was near the gel point and defined as printable material. Based on this research, GelMA with MTGase system could reach this goal. Tailoring DM in GelMA chains could control the amount of lysine groups in the chains, which contributes to the enzymatic crosslinking so that the system may be controlled near the gel point.

# Reference


1. Abouna, G.M. Organ shortage crisis: problems and possible solutions. in Transplantation proceedings. 2008. Elsevier.
2. Ikada, Y., Tissue engineering: fundamentals and applications. Vol. 8. 2011: Academic Press.
3. Wüst, S., R. Müller, and S. Hofmann, Controlled positioning of cells in biomaterials—approaches towards 3D tissue printing. Journal of functional biomaterials, 2011. 2(3): p. 119-154.
4. Gu, B.K., et al., 3-dimensional bioprinting for tissue engineering applications. Biomaterials research, 2016. 20(1): p. 12.
5. Murphy, S.V. and A. Atala, 3D bioprinting of tissues and organs. Nature biotechnology, 2014. 32(8): p. 773-785.
6. Jungst, T., et al., Strategies and molecular design criteria for 3D printable hydrogels. Chem. Rev, 2016. 116(3): p. 1496-539.
7. Hölzl, K., et al., Bioink properties before, during and after 3D bioprinting. Biofabrication, 2016. 8(3): p. 032002.
8. Atala, A. and J.J. Yoo, Essentials of 3D biofabrication and translation. 2015: Academic Press.
9. Peppas, N.A., et al., Hydrogels in biology and medicine: from molecular principles to bionanotechnology. Advanced materials, 2006. 18(11): p. 1345-1360.
10. Gaetani, R., et al., Cardiac tissue engineering using tissue printing technology and human cardiac progenitor cells. Biomaterials, 2012. 33(6): p. 1782-1790.
11. Khalil, S. and W. Sun, Bioprinting endothelial cells with alginate for 3D tissue constructs. Journal of biomechanical engineering, 2009. 131(11): p. 111002.
12. Brandl, F., F. Sommer, and A. Goepferich, Rational design of hydrogels for tissue engineering: impact of physical factors on cell behavior. Biomaterials, 2007. 28(2): p. 134-146.
13. DeForest, C.A. and K.S. Anseth, Advances in bioactive hydrogels to probe and direct cell fate. Annual review of chemical and biomolecular engineering, 2012. 3: p. 421-444.

14. Markstedt, K., et al., 3D bioprinting human chondrocytes with nanocellulose–alginate bioink for cartilage tissue engineering applications. Biomacromolecules, 2015. 16(5): p. 1489-1496.
15. Park, J.Y., et al., A comparative study on collagen type I and hyaluronic acid dependent cell behavior for osteochondral tissue bioprinting. Biofabrication, 2014. 6(3): p. 035004.
16. Duan, B., et al., 3D bioprinting of heterogeneous aortic valve conduits with alginate/gelatin hydrogels. Journal of biomedical materials research Part A, 2013. 101(5): p. 1255-1264.
17. Shanjani, Y., et al., A novel bioprinting method and system for forming hybrid tissue engineering constructs. Biofabrication, 2015. 7(4): p. 045008.
18. Klotz, B.J., et al., Gelatin-methacryloyl hydrogels: towards biofabrication-based tissue repair. Trends in biotechnology, 2016. 34(5): p. 394-407.
19. Wang, X., et al., Generation of three-dimensional hepatocyte/gelatin structures with rapid prototyping system. Tissue engineering, 2006. 12(1): p. 83-90.
20. Yan, Y., et al., Fabrication of viable tissue-engineered constructs with 3D cell-assembly technique. Biomaterials, 2005. 26(29): p. 5864-5871.
21. Zhang, T., et al., Three-dimensional gelatin and gelatin/hyaluronan hydrogel structures for traumatic brain injury. Journal of bioactive and compatible polymers, 2007. 22(1): p. 19-29.
22. Yan, Y., et al., Direct construction of a three-dimensional structure with cells and hydrogel. Journal of bioactive and compatible polymers, 2005. 20(3): p. 259-269.
23. Yue, K., et al., Synthesis, properties, and biomedical applications of gelatin methacryloyl (GelMA) hydrogels. Biomaterials, 2015. 73: p. 254-271.
24. Schuurman, W., et al., Gelatin-methacrylamide hydrogels as potential biomaterials for fabrication of tissue-engineered cartilage constructs. Macromolecular bioscience, 2013. 13(5): p. 551-561.
25. Du, Y., et al., Directed assembly of cell-laden microgels for fabrication of 3D tissue constructs. Proceedings of the National Academy of Sciences, 2008. 105(28): p. 9522-9527.

26. Yeh, J., et al., Micromolding of shape-controlled, harvestable cell-laden hydrogels. Biomaterials, 2006. 27(31): p. 5391-5398.
27. Nichol, J.W., et al., Cell-laden microengineered gelatin methacrylate hydrogels. Biomaterials, 2010. 31(21): p. 5536-5544.
28. Billiet, T., et al., The 3D printing of gelatin methacrylamide cell-laden tissue-engineered constructs with high cell viability. Biomaterials, 2014. 35(1): p. 49-62.
29. Zhao, L., et al., A novel smart injectable hydrogel prepared by microbial transglutaminase and human-like collagen: Its characterization and biocompatibility. Materials Science and Engineering: C, 2016. 68: p. 317-326.
30. Kieliszek, M. and A. Misiewicz, Microbial transglutaminase and its application in the food industry. A review. Folia microbiologica, 2014. 59(3): p. 241-250.
31. Wilson, S.A., et al., Shear-Thinning and Thermo-Reversible Nanoengineered Inks for 3D Bioprinting. ACS applied materials & interfaces, 2017.
32. Grabowska, I., et al., Comparison of satellite cell-derived myoblasts and C2C12 differentiation in two-and three-dimensional cultures: changes in adhesion protein expression. Cell biology international, 2011. 35(2): p. 125-133.
33. Langer, R. and J.P. Vacanti, Tissue engineering. Science, 1993. 260(5110): p. 920-926.
34. Ma, L., et al., Collagen/chitosan porous scaffolds with improved biostability for skin tissue engineering. Biomaterials, 2003. 24(26): p. 4833-4841.
35. Chen, A.A., et al., Humanized mice with ectopic artificial liver tissues. Proceedings of the National Academy of Sciences, 2011. 108(29): p. 11842-11847.
36. Chia, H.N. and B.M. Wu, Recent advances in 3D printing of biomaterials. Journal of biological engineering, 2015. 9(1): p. 4.
37. Langer, R., Biodegradable polymer scaffolds for tissue engineering. Nat. Biotechnol, 1994.
38. Loh, Q.L. and C. Choong, Three-dimensional scaffolds for tissue engineering applications: role of porosity and pore size. Tissue Engineering Part B: Reviews, 2013. 19(6): p. 485-502.
39. Yang, S., et al., The design of scaffolds for use in tissue engineering. Part I. Traditional factors. Tissue engineering, 2001. 7(6): p. 679-689.

40. Yeong, W.-Y., et al., Rapid prototyping in tissue engineering: challenges and potential. Trends in biotechnology, 2004. 22(12): p. 643-652.
41. Do, A.V., et al., 3D printing of scaffolds for tissue regeneration applications. Advanced healthcare materials, 2015. 4(12): p. 1742-1762.
42. Hull, C.W., Apparatus for production of three-dimensional objects by stereolithography. 1986, Google Patents.
43. Nakamura, M., et al., Biomatrices and biomaterials for future developments of bioprinting and biofabrication. Biofabrication, 2010. 2(1): p. 014110.
44. Barron, J., et al., Biological laser printing: a novel technique for creating heterogeneous 3-dimensional cell patterns. Biomedical microdevices, 2004. 6(2): p. 139-147.
45. Boland, T., et al., Application of inkjet printing to tissue engineering. Biotechnology journal, 2006. 1(9): p. 910-917.
46. Mironov, V., Printing technology to produce living tissue. 2003, Taylor & Francis.
47. Cui, X., et al., Thermal inkjet printing in tissue engineering and regenerative medicine. Recent patents on drug delivery & formulation, 2012. 6(2): p. 149-155.
48. Odde, D.J. and M.J. Renn, Laser-guided direct writing for applications in biotechnology. Trends in biotechnology, 1999. 17(10): p. 385-389.
49. Geckil, H., et al., Engineering hydrogels as extracellular matrix mimics. Nanomedicine, 2010. 5(3): p. 469-484.
50. Friess, W., Collagen–biomaterial for drug delivery. European Journal of Pharmaceutics and Biopharmaceutics, 1998. 45(2): p. 113-136.
51. Smith, C.M., et al., Three-dimensional bioassembly tool for generating viable tissue-engineered constructs. Tissue engineering, 2004. 10(9-10): p. 1566-1576.
52. Michon, C., G. Cuvelier, and B. Launay, Concentration dependence of the critical viscoelastic properties of gelatin at the gel point. Rheologica Acta, 1993. 32(1): p. 94-103.
53. LeRoux, M.A., F. Guilak, and L.A. Setton, Compressive and shear properties of alginate gel: effects of sodium ions and alginate concentration. Journal of biomedical materials research, 1999. 47(1): p. 46-53.

54. Zhu, J., Bioactive modification of poly (ethylene glycol) hydrogels for tissue engineering. Biomaterials, 2010. 31(17): p. 4639-4656.
55. Hockaday, L., et al., Rapid 3D printing of anatomically accurate and mechanically heterogeneous aortic valve hydrogel scaffolds. Biofabrication, 2012. 4(3): p. 035005.
56. Skardal, A. and A. Atala, Biomaterials for integration with 3-D bioprinting. Annals of biomedical engineering, 2015. 43(3): p. 730-746.
57. Das, S., et al., Enhanced redifferentiation of chondrocytes on microperiodic silk/gelatin scaffolds: toward tailor-made tissue engineering. Biomacromolecules, 2013. 14(2): p. 311-321.
58. Wüst, S., et al., Tunable hydrogel composite with two-step processing in combination with innovative hardware upgrade for cell-based three-dimensional bioprinting. Acta biomaterialia, 2014. 10(2): p. 630-640.
59. Malda, J., et al., 25th anniversary article: engineering hydrogels for biofabrication. Advanced Materials, 2013. 25(36): p. 5011-5028.
60. Mezger, T.G., The rheology handbook: for users of rotational and oscillatory rheometers. 2006: Vincentz Network GmbH & Co KG.
61. Yilmaz, M.T., D. SERT, and M.K. DEMIR, Rheological properties of Tarhana soup enriched with whey concentrate as a function of concentration and temperature. Journal of texture studies, 2010. 41(6): p. 863-879.
62. Koocheki, A., et al., The rheological properties of ketchup as a function of different hydrocolloids and temperature. International journal of food science & technology, 2009. 44(3): p. 596-602.
63. Rezende, R.A., P.J. Bártolo, and A. Mendes, Rheological behavior of alginate solutions for biomanufacturing. Journal of applied polymer science, 2009. 113(6): p. 3866-3871.
64. Axpe, E. and M.L. Oyen, Applications of alginate-based bioinks in 3D bioprinting. International journal of molecular sciences, 2016. 17(12): p. 1976.
65. Melchels, F.P., et al., Development and characterisation of a new bioink for additive tissue manufacturing. Journal of Materials Chemistry B, 2014. 2(16): p. 2282-2289.

66. You, F., X. Wu, and X. Chen, 3D Printing of Porous Alginate/gelatin Hydrogel Scaffolds and Their Mechanical Property Characterization. International Journal of Polymeric Materials and Polymeric Biomaterials, 2016(just-accepted).
67. Fuchs, S., et al., Transglutaminase: New insights into gelatin nanoparticle cross-linking. Journal of microencapsulation, 2010. 27(8): p. 747-754.
68. Kuwahara, K., et al., Cell delivery using an injectable and adhesive transglutaminase–gelatin gel. Tissue Engineering Part C: Methods, 2009. 16(4): p. 609-618.
69. Chen, P.-Y., et al., Fabrication of large perfusable macroporous cell-laden hydrogel scaffolds using microbial transglutaminase. Acta biomaterialia, 2014. 10(2): p. 912-920.
70. Fuchsbauer, H.-L., et al., Influence of gelatin matrices cross-linked with transglutaminase on the properties of an enclosed bioactive material using β-galactosidase as model system. Biomaterials, 1996. 17(15): p. 1481-1488.
71. Irvine, S.A., et al., Printing cell-laden gelatin constructs by free-form fabrication and enzymatic protein crosslinking. Biomedical microdevices, 2015. 17(1): p. 16.
72. Guvendiren, M., et al., Designing biomaterials for 3D printing. ACS biomaterials science & engineering, 2016. 2(10): p. 1679-1693.
73. Bertassoni, L.E., et al., Direct-write bioprinting of cell-laden methacrylated gelatin hydrogels. Biofabrication, 2014. 6(2): p. 024105.
74. Yi, J., et al., Influence of transglutaminase-induced cross-linking on properties of fish gelatin films. Journal of food science, 2006. 71(9): p. E376-E383.
75. D O'Connell, C., et al., Development of the Biopen: a handheld device for surgical printing of adipose stem cells at a chondral wound site. Biofabrication, 2016. 8(1): p. 015019.
76. Williams, C.G., et al., Variable cytocompatibility of six cell lines with photoinitiators used for polymerizing hydrogels and cell encapsulation. Biomaterials, 2005. 26(11): p. 1211-1218.
77. Shirahama, H., et al., Precise tuning of facile one-pot gelatin methacryloyl (GeLMA) synthesis. Scientific Reports, 2016. 6.

78. McDermott, M.K., et al., Mechanical properties of biomimetic tissue adhesive based on the microbial transglutaminase-catalyzed crosslinking of gelatin. Biomacromolecules, 2004. 5(4): p. 1270-1279.
79. Li, H., S. Liu, and L. Lin, Rheological study on 3D printability of alginate hydrogel and effect of graphene oxide. International Journal of Bioprinting, 2016. 2(2).
80. Bae, H.J., et al., Effects of transglutaminase-induced cross-linking on properties of fish gelatin–nanoclay composite film. Food chemistry, 2009. 114(1): p. 180-189.
81. Zhao, Y., et al., The influence of printing parameters on cell survival rate and printability in microextrusion-based 3D cell printing technology. Biofabrication, 2015. 7(4): p. 045002.
82. Ng, W.L., W.Y. Yeong, and M.W. Naing, Polyelectrolyte gelatin-chitosan hydrogel optimized for 3D bioprinting in skin tissue engineering. International Journal of Bioprinting, 2016. 2(1).
83. Chung, J.H., et al., Bio-ink properties and printability for extrusion printing living cells. Biomaterials Science, 2013. 1(7): p. 763-773.
84. Rutz, A.L., et al., A multimaterial bioink method for 3D printing tunable, cell-compatible hydrogels. Advanced Materials, 2015. 27(9): p. 1607-1614.